MASTER'S THESIS

Jiaxi XIANG

Aging and Humidity Effects of Hydrocarbon Gas Sensor Based on Carbon Nanotubes Functionalized with Metal Oxide Nanocrystals

Supervisors:
Professor Knut E. Aasmundtveit
Asc. Professor Igor Paprotny
Dr. Michela Sainato
Divan, Ralu Nana Silvia

July 3, 2017

Preface

This Thesis is the description of my master's project, carried out of the University College of Southeast Norway and collaborated with University of Illinois at Chicago during 2017. All experimental work have been done by myself at Center for Nanoscales Materials of Argonne National Laboratory and Micro-mechatronic Systems Laboratory of UIC, except for the TEM and SEM imaging, which was done at CNM of ANL by Divan, Ralu Nana Silvia.

My supervisors have guided me through this project in an excellent way, and all deserve my greatest thanks: Igor Paprotny, Knut E. Aasmundtveit, Michela Sainato and Divan Ralu Nana Silvia.

I also want to thank Lilianan and Ralu for all the help in the cleanroom, Czaplewski, David for teaching me how to use the RIE and all the memebers of the MSL group for the inspiring weekly meetings.

Abstract

With the enhanced greenhouse effect and the increasing pollutants in the air, gas sensors applied in door or outdoors are in great demand. A hetero-structure gas sensors based on Multi-walled Carbon nanotubes (MWCNT) functionalized with metal oxide (MOX) nanoparticles are fabricated, which can be operated at room temperature with low power consumption. ZnO and TiO_2 nanoparticles were deposited on MWCNT by Atomic Layer Deposition (ALD) at different temperatures from 175 ℃ to 220 ℃/225 ℃. The characteristics of hydrocarbon gas sensor fabricated at different temperatures were analyzed. MOX- MWCNT sensors have good sensitivities under low concentration (10ppm) of methane. Since this sensor is supposed to be used in common conditions at room temperature (RT) and room restive humidity (RH), aging process was in room relative humidity at RT. Humidity effects were investigated by comparing the performance of sensors at 2% RH and 50% RH. The humidity is strong effect on MOX-MWCNT sensor.

Contents

List of Tables

Chapter 1

Introduction

Hydrocarbon is a compound composed of only carbon and hydrogen. The most obvious danger of most hydrocarbons is highly flammable. As an important greenhouse gas, the green house effect is more than 20 times greater than the equivalent mass of carbon dioxide. Moreover, benzene and many aromatic compounds are possible carcinogens. [1]. Therefore, hydrocarbon gas sensors are widely used to monitor the environment in industry.

Gas sensors, or chemical sensors are commonly based on semiconductor metal-oxide. SnO_2, In_2O_3, ZnO, *etc.* are the typical semiconductor metal oxide material for gas sensor. [2]. Both gas absorption and formation of oxygen vacancies on the metal oxide layer can induce a space charge region, which results with the conductivity change of the sensor. [3].

The sensitivity (detection of gas concentrations at the ppm level) and selectivity (detection of specific gases in a mixed gas environment) are two of the basic criteria for good and efficient gas sensing systems. However, semiconductor metal oxides mostly suffer from a lack of gas selectivity.[4]. Another drawback of metal oxide gas sensors are commonly operated at high temperature.

Carbon nanotubes (CNTs) becomes one of the most popular materials of gas sensor in recent years, since nanostructured materials present new opportunities for enhancing the properties and performance of gas sensors. With the large surface to volume ratio, presence of defects, and porous structure, CNTs provide highly effective binding sites for gas molecule, which enables the absorption of gas molecule at room temperature. [5]. However, only several strongly oxidizing gases and strongly reducing gases such as oxygen (O_2), nitrogen dioxide (NO_2), ammonia (NH_3), and sulfur dioxide (SO_2) can be detected by the intrinsic carbon nanotubes.

To solve the drawbacks of MOX and CNTs, these two kinds of materials can be employed in one structure. Metal oxide can be doped to CNT or deposited on CNTs. M.T.Humayun et al [6] fabricated a novel chemorsistive CH_4 based on Multi-walled

Carbon nanotubes functionalized with SnO_2 nanoparticles, which can be used to sensor Methane (CH_4) with high sensitivity at room temperature. [6].

The long-term stability of sensors is critical for sensor's performance as well. A lot of elements will affect the reaction on the surface of MOX, such as natural properties of base materials, surface areas and microstructure of sensing layers, surface additives, temperature and humidity, etc. [7]. For example, water molecule can be absorbed by MOX surface, which will affect the reaction between target gas molecule and the MOX surface. MWCNT can also absorb the Oxygen and water vapor, affecting the performance of sensors. Therefore, investigation of aging effects of gas sensor, like UV exposure [8] and humidity, is necessary to avoid the influence of environmental changes.

This study focuses on fabrication and investigation of aging and humidity effect of the hydrocarbon sensor based on carbon nanotubes functionalized with metal oxide nanocrystals. ZnO and TiO_2 nanoparticles were employed in the hetero structure chemiresistive sensors. MOX particles were deposited on CNT through atomic layer deposition (ALD).

Chapter 2

Gas Sensor Technologies

2.1 Types of Gas Sensors

The atmospheric air we live in contains numerous kinds of chemical species. Some of them are crucial for human life like oxygen. However, some other kinds of gases, natural or produced in industry, are hazardous for human directly or indirectly. For example, methane, commonly used as fuels, will absorb the heat from the earth resulting greenhouse phenomenon. For toxic gases, volatile organic compounds (VOCs) and other kinds of air pollutants, like toluene and benzene, their standards and guidelines have been set by various organizations in industrial settings. Therefore, Gas sensors, the device transforming the chemical information of particular gas into readable signal, are widely used to monitor the environment in industry or household to ensure the safety. The gas sensors can be classified into different types according to different functional materials, such as semiconductors, ionic conductors, piezoelectric crystals, catalytic combustion catalysts, optical fibers, etc. [4, 9]

2.1.1 Semiconductor gas sensor

Semiconductor gas sensors (metal oxide sensor) are electrical conductivity sensors, which can be divided into two main types: resistor type and MISFET (Metal-Insulator-Semiconductor-Field Effect Transistor). The resistive gas sensor showed in Figure.1 contains an active sensing layer, electrodes and heating elements.

When the gas reacts on the metal oxide surface (oxidation or reduction), the conductivity or resistivity of the active sensing layer changes from the baseline value. By monitoring the changes of resistance (current), the gas concentration can be detected based on calibration equations. [10].

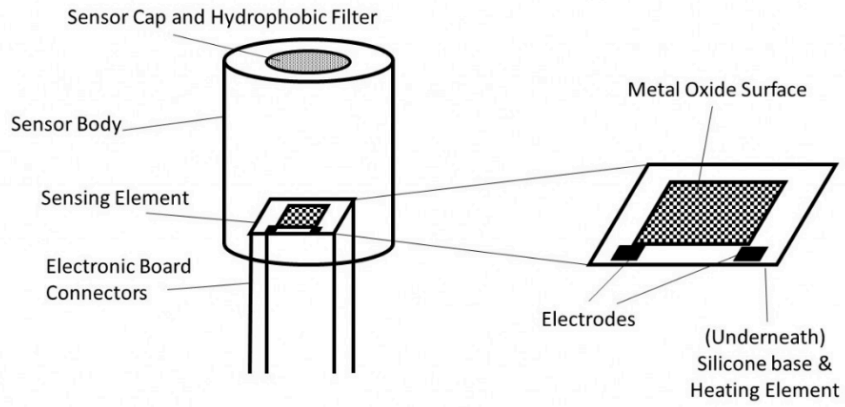

Figure 1 Structure of resistive gas sensor [11]

SnO_2, ZnO, WO_3 and TiO_2 are usually used as sensing materials for semiconductor gas sensors, which is sensitive to inflammable gases, CO, H_2S, NH_3, NO, etc. The Figure. 2 illustrate the reaction on the MOX surface.

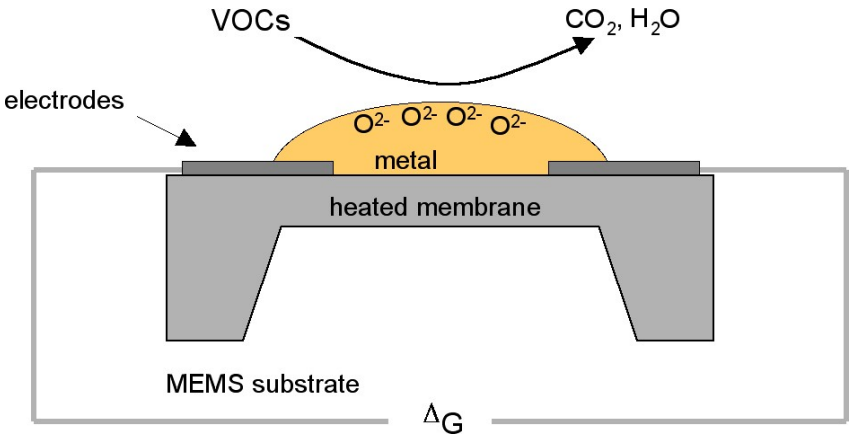

Figure 2 Sensing principle of semiconductor metal oxide [48]

For n-type MOX (SnO2, ZnO, etc.), the electrons are majority carriers, which will be transformed from the surface to the physically adsorbed oxygen in the air. At room temperature, this process is extremely slow. When the MOX is heated at high temperature (e.g. 400°C for SnO2), electrons in valence band are excited and transfer to conductive band. Free electrons will flow through the grain boundary of the MOX crystal. Attracting free electrons of MOX, oxygen ions O^-, O_2^- or O^{2-} will be generated on the surface depending on the temperature. As a consequent, potential barrier at the grain boundaries is built, which prevents electron flow, decreasing the conductivity of MOX. Once the heated MOX is exposed under reducing gas, such as

CO, H2, CH4, VOCs etc., the reducing gas molecule will react with the oxygen ions. (e.g. In Figure. 2)

$$C_6H_6 \text{ (benzene)} + O_2^- \longrightarrow CO_2 + H_2O$$

The freed electrons can return to the conductive band, decreasing the sensor resistance. On the contrary, the resistance increases under oxidizing gases. For p-type MOX, the case is opposite to that for n-type in that the majority carrier is holes and the electron transfer is in contrast with that in n-type MOX.

Most of sensors based on metal oxide semiconductors are operated at high temperature at the range from 200-450 ℃ due to the reaction of oxygen ions.

For MISFET-type gas sensors, various kinds of material can be introduced into gas sensitive gate, allowing various gases detection. [9]. H_2, H_2O, NO_2, etc. are the target gas of this kind of sensors. A novel e Pd/oxide/GaAs sensor based on a MISFET was fabricated by Kun-Wei Lin[12] to detector the Hydrogen with high-speed and high-sensitivity.

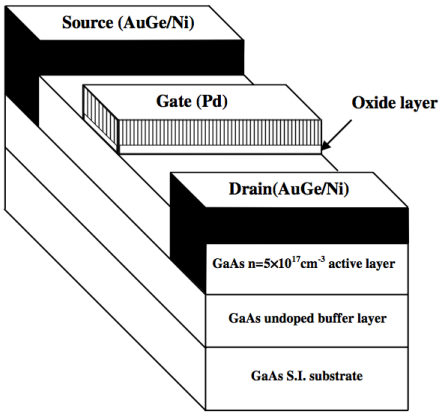

Figure 3 Cross section of MISFET gas sensor[12]

Based on the target gas concentration, the threshold voltage in the gate layer changes, resulting in a change in the drain current.

Semiconductor gas sensors are one of the kinds of low cost sensors due to their simplicity and scalability. However, it can be unreliable at high relative humidity and varying temperatures since metal oxide materials are sensitive to water vapor.[10]. No-target gases may also absorb on the oxide surface leading incorrect measurements because of the poor selectivity of metal oxide when the operating temperature is high.

2.1.2 Gas sensor based on catalytic combustion

The typically monitored gas of both of infrared and catalytic gas sensor includes methane, ethane, propane, hexane, etc. The construction of the catalytic sensor is shown in Figure. 4 a). [13].

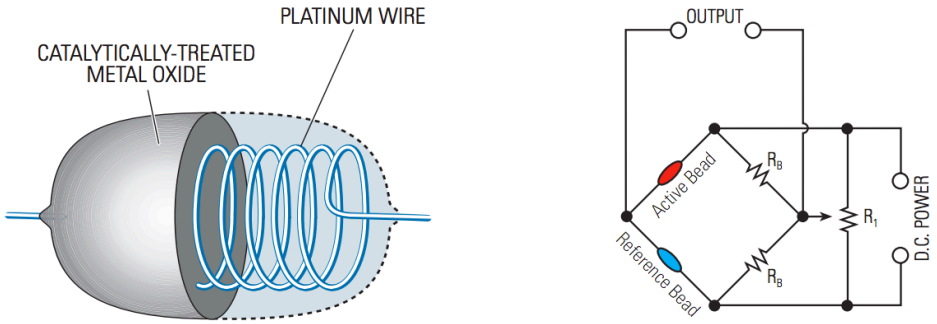

a) b)

Figure 4 a) Catalytic combustion types b) catalytic gas sensor Wheatstone bridge

The circuit shown in Fig. 4 b) is the circuit for measuring an unknown resistance by comparing it with known resistances.

The sensor constant of a pair of platinum coils with a catalyst, which enables the flameless combustion of target gas on the surface of the element. The Wheatstone bridge keeps balance and has no offset signal. With the rising of temperature caused by the heat of burning, the resistance of platinum coil increases, breaking the balance of Balance Bridge. The Platinum has a large coefficient of temperature resistance (Ct), which is linear between 500°C to1000°C (in the range of working temperature). Therefore, an electrical signal proportional to the concentration of combustible gas is output.

Catalytic detector is long lived with life-cycle cost, simply operated and easily calibrated. In addition, the catalytic gas sensors can be used to detect gases, which cannot be detected through infrared absorption. The obvious drawback of this sensor is the requirement of working environment since oxygen is necessary for catalytic combustion. [16]

2.1.3 Gas Sensor based on Infrared spectroscopy

The infrared detector is based on selected absorption of near-infrared spectroscopy for different gas molecule. Combining with the Lambert-Beer Law, which can be

illustrated by equation (a), the identification and concentration of gases can be determined. [15].

The absorption of infrared spectroscopy occurs at resonant frequencies. The part of energies having the same frequency with the natural frequency of molecule will be absorbed, contributing to more vigorous vibration. Since the energies are affected by the shape of the molecule potential energy surfaces, the masses of the atoms, and the associated vibronic coupling, different gases with unique molecule structures show unique gas absorption "fingerprints" in infrared spectroscopy.[14]. The functional groups in various frequencies are shown in Figure.5, where the wavenumber is 1/ wavelength.

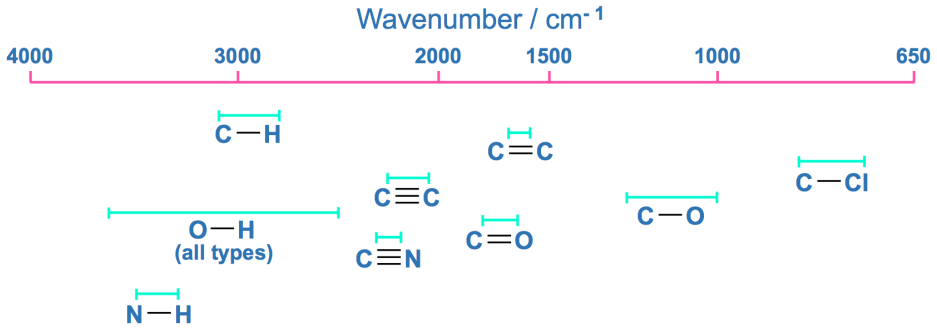

Figure 5 Funtional groups at different frequencies

According to the Bouguer Lambert-Beer Law, the absorbance

$$A = -log_{10}\frac{I_t}{I_0} = log_{10}\frac{1}{T} = K \cdot l \cdot c \qquad \text{(a)}$$

$$c = \frac{1}{K \cdot l} log_{10}\frac{1}{T} \qquad \text{(b)}$$

Where A is absorbance, I_t is the intensity of the incident light, I_0 is the intensity of the transmitted light, T is transmittance, K is molar attenuation coefficient, l is path length of the sample and c is the concentration of target gas.

Two detection methods can be employed for IR sensors. The energy will be obtained by gas molecule when this molecule absorbs the radiation of IR, whose frequency consists with the natural frequency of the gas molecule. Consequently, the temperature increases in proportion to the gas concentration, which can be detected by the sensor.

On the other hand, decrease in the original source strength accompany with the radiation absorption. This radiation energy decrease can be detected as a signal as well.

The main advantage of infrared gas sensor is that the sensor does not directly interact with gases, having immunity to contamination and poisoning. Unlike the catalytic gas sensor, it can be operated either in no oxygen or enriched oxygen. In addition, this kind of sensor can be operated in continuous presence of gas.[IR and catalytic]. However, there are still some limits of IR gas sensor. The gases cannot be detected if they are inactive to IR. The fixed environment temperature (70°C) for sensor operation limits the application of IR gas sensor. Higher spare parts cost and higher maintenance cost compared with catalytic gas sensor are main drawbacks as well.

2.2 Hydrocarbon gas sensors

There are many different types of hydrocarbons presented in the environment, whose main characteristics are listed in the Table 1. This study focuses on the first three in the table, especially on the methane.

Table 1 Properties of some hydrocarbons

Molecule	**Molecule weight (g/mol)**	**Density at 25℃ (g/cm^3)**	**Boiling temperature(c)**	**Solubility at 25 ℃**
Methane	16	0.423	-161.5	0.0227
Benzene	78.1	0.874	80.1	1.78
Toluene	92.1	0.862	110.6	0.53
Ethylbenzene	106.2	0.863	136.2	0.161
o- Xylene	106.2	0.876	144.4	0.171
m-Xylene	106.2	0.860	139.1	0.161
p- Xylene	106.2	0.857	138.4	0.181

Methane (CH_4) is another critical greenhouse gas expect Carbon Dioxide (CO_2). However, green house effect is more than 20 times greater than the equivalent mass of carbon dioxide. [17]. Benzene (C_6H_6) is an important organic chemical compound, which is toxic and can increase the risk of cancer. As most of the hydrocarbons, Toluene ($C_6H_5CH_3$) is highly flammable at room temperature. All of them are threatening the safety and health of human. The EPA (United States Environmental

Protection Agency) seeks to reduce the VOC and Methane emissions by 40-45% by 2025.

Chemiresistive gas sensor and Infrared point sensors are commonly used to detect hydrocarbons. Comparing with IR sensors, Chemiresitive sensors has lower cost, enabled lower operating temperature and easier to be install. Therefore, this work focuses on chemiresistor for hydrocarbon gas detection.

2.2.1 Sensing Principle of Chemiresistive Gas Sensor

As typical resistive sensor, the some structures of chemiresistive gas sensor are shown in Figure 6, which is similar with semiconductor sensors. Metal oxide semiconductors are most commonly used in chemiresistive sensors.

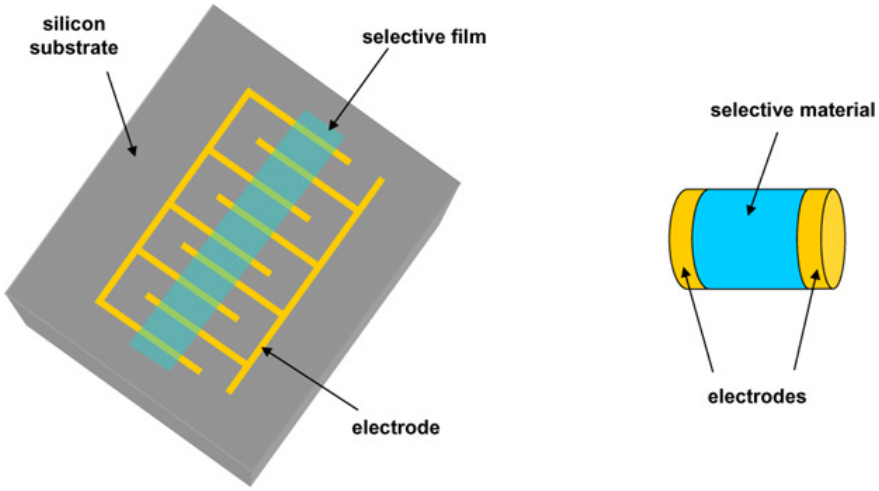

Figure 6 Typical chemiresistor sensors for hydrocarbon detection [11]

The chemiresistive sensor consists of electrodes and active sensing layer between electrodes. Gas absorption and formation of oxygen vacancies on sensing layer can induce a space charge region, which results with the conductivity and resistivity change of the sensor. By measuring the resistance (current) of the sensor, the gas molecule can be detected.

2.2.2 Characteristics of chemiresistive sensors

The typical sensor response curve is the resistance vs. time characteristic of the sensor. Figure. 7 illustrates the sensor response of a chemiresistive gas sensor exposed under methane every 10 minutes.

There are several parameters of chemiresistive sensors to characterize the sensor response curve.[9]

Sensitivity: the sensitivity *S* can be defined in different ways. There are two main definition of *S*.

1) $S = \frac{R_0}{R_S}$, where R_0 is the resistance of sensor in the air, R_S is the resistance in the target gas. The higher value of S indicates the better sensitivity of the sensor.
2) $S(\%) = \frac{R_0 - R_S}{R_0} * 100$, S is the ratio of the resistance difference to the resistance in air.

Response time: It is the time for sensors to response to a step concentration change from zero to a certain concentration value. [19]. The time is measured from the edge of target gas coming to the 90% of the final value (T90) of the resistance during the exposure under target gas (Figure 7). Less response time indicates better performance of the sensor.

Recovery Time: It is the time takes for the sensor signal to return to the baseline value after a step concentration of analyzing gas change from certain concentration value to zero. Small value of recovery time is necessary to a good sensor to ensure the quick recover from last circle.

Selectivity: Most of chemiresisttive gas sensors are sensitive to more than one gas. The selectivity refers to the characteristic that determines whether sensors can distinguish a specific gas form a group of analyzing gases. It is defined as following:

$$Selectivity = \frac{sensitivity\ for\ interfering\ gases}{sensitivity\ for\ target\ gas}$$

Stability: it is the ability of a sensor to provide reproducible results for a certain period of time. This includes retaining the sensitivity, selectivity, response and recovery time.

Those parameters depend on various factors, such as sensor materials, reaction between gas molecule and the active sensing layer, the operating conditions etc. [20-22].

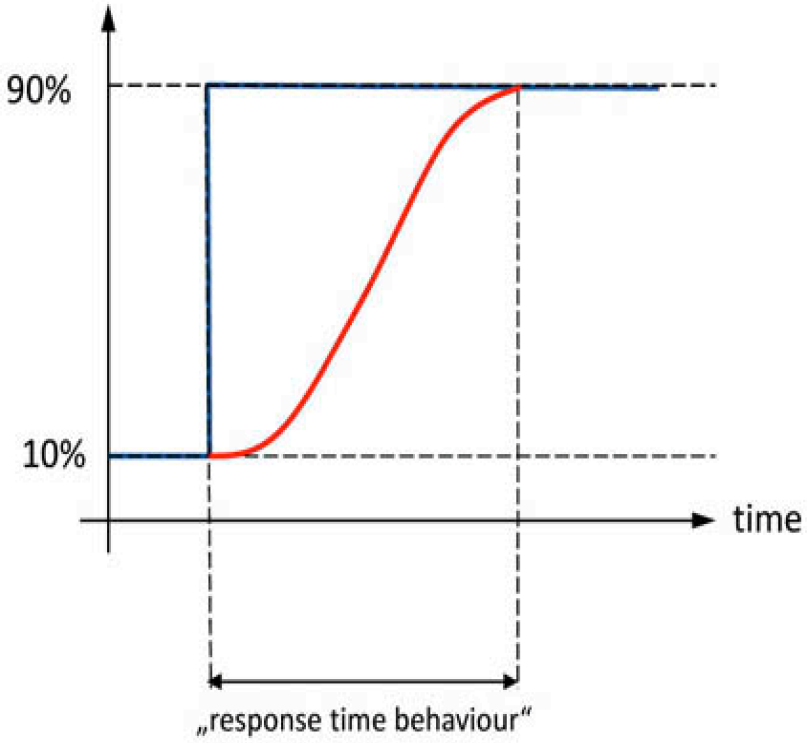

Figure 7 Sensor response of chemiresistor under methane

2.2.3 Materials

Various materials can be used as active sensing layer of chemiresistive gas sensor, which can be generally classified to two main types. One of them is Semiconductor Metal oxide. Another is non-oxide material including carbon nanotubes, polymer and metal.

2.2.3.1 Chemiresistive gas sensor based on Metal Oxide (MOX)

Some metal oxides with semiconductor characteristics can interact with target molecule on their surface, leading the change of conduction. The principle is illustrated in semiconductor sensors part. In general, sensors based on metal oxide have high response of pollutant gases and short response and recovery time. Different metal oxides are sensitive to different gases. The metal oxide commonly used and their corresponding target gases are listed in Table 2. [9, 23-25]

Table 2 Semiconductor metal oxides corresponding with target gases [9]

Base material	***Additives***	***Target gas***
SnO_2	Pt, Ag, Pd, Fe, Au, In, Ru, CeO_2, CuO, Bi_2O_3	CO, CH_4, SO_2, N_2O, CO_2, NO_2, CH_3OH, C_2H_5OH, C_3H_8, H_2, H_2S, NH_3, C_nH_{2n+2}
WO_3	Mg, Zn, Mo, Re, Au, Pd	NO_2, NH_3, H_2S, O_3
ZnO	Al, Sn, Cu, Pd, Fe_2O_3	NH_3, H_2, NO_2, LPG, CH_4, CO, CH_3OH, C_2H_5OH, C_3H_7OH
CuO	SnO_2	CO, ethanol, H_2S
Cr_2O_3	TiO_2	NO_2, O_2, NH_3
V_2O_5	Fe_2O_3, SnO_2, TiO_2	NO_2, NH_3, C_2H_5OH, Toluene, Propanol, Butylamines
TiO_2	La, Pt, Cr2O3, WO_3	CH_3OH, C_2H_5OH, C_3H_7OH, O_2, H_2, NH_3, NO_2
Fe_2O_3	Au, Zn	Methane, Propane, Benzene, Toluene
Al_2O_3	Al, SiO2/Si	Humidity, CH_4, NH_3
Ca_2O_3	SnO_2, Pd, Ta_2O_5, WO_3, NiO	O_2, CO, CH_4, NO, NH_3
NiO	Li, TiO_X	H_2, HCHO, CH_4, CH_3COOH, CO, NO_2
In_2O_3	MoO_3, Au, Al, SnO_2	O_3, NO_2, H_2, CO, C_3H_8, H_2S, CO_2, SO_2, NH_3, Ethanol
CdO	$ZnFe_2O_4$	Ethanol

The information from the table above illustrate one metal oxide sensor is sensitive to many gases, indicating the selectivity is a vital issue for metal oxide gas sensors. Adding proper promoters showed in the table is one of the common methods to improve the selectivity of MOX gas sensors. [26].

Nanoscale technologies present new opportunities for enhancing the performance of the MOX gas sensors. Since the gas adsorption occurs mainly on the surface of metal oxide, the gain size and the area of active sensing layer are the critical parameters affecting the sensor performance. With high surface to volume ratio, metal oxide

nanoparticles provide large interface to gas molecule. Therefore, for the same metal oxide, the smaller the nanomaterials are, the better performance the sensor is.

There are different nanostructures of metal oxide are used for gas sensing:

Expect the high surface to volume ratio, the nanowires of metal oxide provide the pathway to the electron transfer, improving the reaction kinetics. Wan et al [27] fabricated ZnO nanowire sensors, which has highly sensitivity for ethanol at a working temperature of 300 C. And Lin et al [28] prepared ZnO nanowire gas sensor on plastic substrate. Employing the UV light, the sensor has good response under lower temperature around 60C, implying lower power consumption.

Compared with nanowires, metal oxide nanotubes have lager surface area contributed by their hollow structure. Lee et *al* [29] fabricated vertically aligned TiO2 nanotube arrays applied to hydrogen gas sensor. The sensor had very short response time (< 1s) and high selectivity for H_2 against NH_3, CO and C_2H_5OH.

Porous single-crystalline nanostructures is idea martial enabling the balance between high response and good stability. Liu et al [30] fabricated a single-crystalline ZnO nanosheets with porous structure by annealing ZnS(en)0.5 (en = ethylenediamine) complex precursor. When this material was employed as sensing layer, the highly sensitivity, short response and recovery time can be obtained.

2.2.3.2 Chemiresistor gas sensor based on CNT

Most of sensors based on metal oxide semiconductor suffer from the poor selectivity and high operating temperature. With the development of nanotechnologies, CNT can be used to solve the dilemma.

Carbon nanotubes can be though as a rolled-up graphene sheets. Therefore, according to the layer of grapheme sheets, CNT can be classified to Single Walled Carbon Nanotubes (SWCNTs) and Multi-walled Carbon nanotubes (MWCNTs). Defects are introduced to the MWCNTs during the formation of MWCNTs. Compared with the multi-wall tube, the single-walled tube has less defects, with a higher uniform consistency. [31] Figure.8 shows the structure of CNT. The different helices and diameters of intrinsic carbon nanotubes determine their electronic structure and reflect the properties of semiconductors or metals at room temperature.[32].

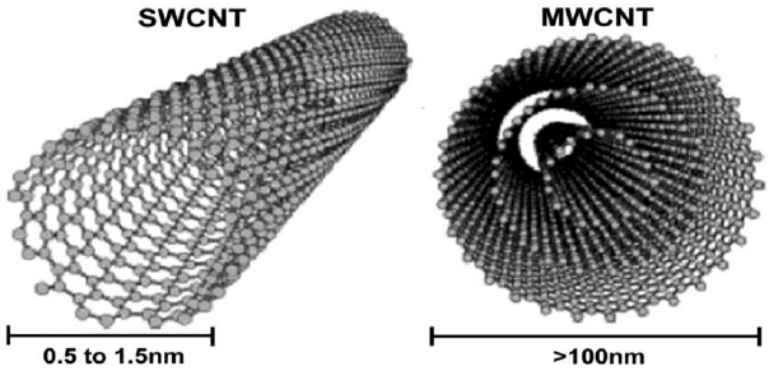

Figure 8 Structures of SWCNT and MWCNT

As shown in Figure 8, Carbon nanotubes have a unique hollow structure, providing extremely large surface to volume ratio. And the hanging keys on the surface enable a strong adsorption capability. There are four potential adsorption sites (seen in Figure. 9) in the CNTs [33] for the adsorption of diverse gases: (1) “internal sites”—the hollow interior of every tube; (2) “interstitial channels”—the hollow channels between individual tubes; (3) “grooves”—the exterior surface of the tubes, where two adjacent parallel tubes meet; and (4) “outside surface”—the curved surface of tubes on the outside of the nanotube bundles.

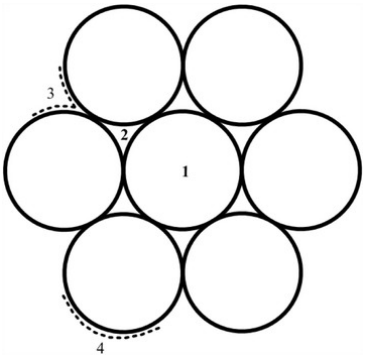

Figure 9 Four potential adsorption sites

Though there are several possible adsorption sites, certain gas molecules could only be adsorbed at given ones due to their own properties.[33] The electronic properties of CNTs are strongly affected by molecule adsorption.[34]

The structure of chemiresistor based on CNT is shown in Figure 10. [35]. CNT meshes deposited between positive and negative electrodes through which current is passing and The binding of analytes on the CNT surface leading charge transfer between the adsorbate and the surface of the CNT and alters its electrical resistance.[36].

The semiconductor-type carbon nanotubes are usually P-type [32], and the majority of carriers are holes. When the carbon nanotubes adsorb the reducing gas, if the charge

transfer occurs, the electrons will enter into the carbon nanotubes and recombine with the holes, resulting in a decrease in the electrical conductivity and a rise in the macro resistance. Similarly, when absorbing oxidizing gases, carbon nanotubes in the electrons are taken away by the gas, the number of holes increases, the conductivity increases, and thus the macro resistance decreases.

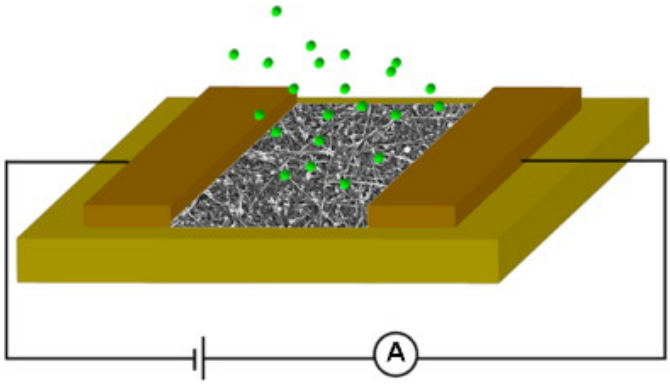

Figure 10 Mechanism of sensors based on CNTs

However, the kinds of gases can be absorbed by CNT are limited. Only several strongly oxidizing gases and strongly reducing gases such as oxygen (O_2), nitrogen dioxide (NO_2), ammonia (NH_3), and sulfur dioxide (SO_2) can be detected by CNT. Therefore, a lot of materials including inorganic metal, metal compound, nonmetallic elements are doped to CNT to improve the sensitivity of CNT based sensors. [37]

2.2.3.3 Chemiresistive gas sensor based on composite nano-structure

MOX- Metal/MOX

To improve the characteristic of sensors, adding proper promoters on metal oxide sensing layer is a traditional way. Promoter (Metal particles, foreign metal oxide) is high active, which make it react with absorbed gas molecule preferentially. The Figure 11 shows the spill-over mechanism. [38]. The cluster on the metal oxide film reacts with the O2 in the air, forming oxygen anions which will spill over to the metal oxide film. The spilled anions are beneficial to the reaction with absorbed oxygen species, increasing the sensitivity to hydrogen and a lowering of the working temperature.

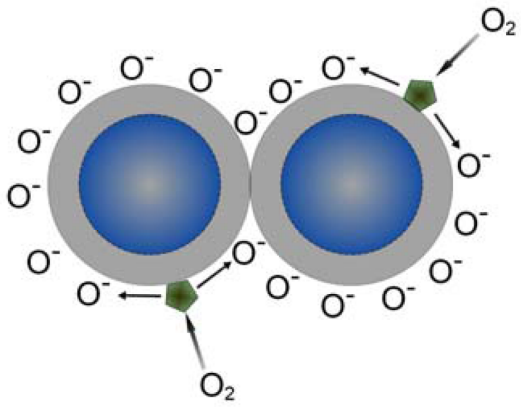

Figure 11 Oxygen ions spill over the metal oxide film

CNT-Metal

D. J. Mowbray et al [39] doped 3D transition metal atom to the defect of CNT and they found Ni doping on the CNT is the most promising candidate for detecting CO in a background of air at room temperature and pressure. As shown in Figure 12, in metal-doped CNT structure, the metal atoms occupy the vacancies of CNT, forming an "active site" where the target gas molecule can be absorbed. The properties of CNT can be change by doping with different dopant.

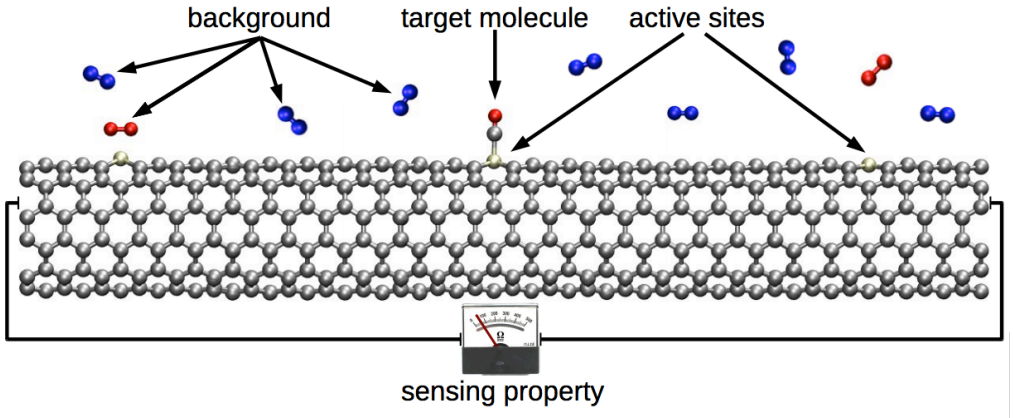

Figure 12 Transition metal atom doped on CNT

MOX-CNT

The material used in this work is Multi Walled CNT functionalized with MOX nanoparticles. In this hetero-structure, metal oxide nanoparticles are employed as photo catalysts, which can absorb light and accelerate the reaction on the surface without any change after each cycle of reaction. Most of the semiconductor photo-catalysts are n-type semiconductor materials, including TiO2, ZnO, SnO2 and CeO2. In Figure 13, [40] the characteristics of TiO2 nanoparticle, the most widely used semiconductor photo catalyst, are illustrated as an example.

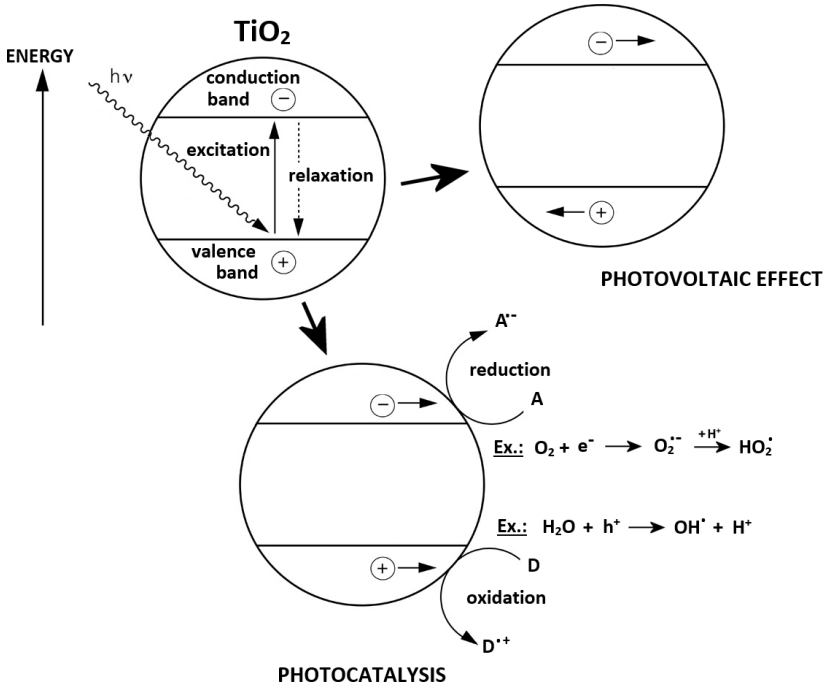

Figure 13 Photo-catalysis mechanism

For TiO_2, the band gap energy w_g between conduction band and valence band is 3.2eV. When energy of photon is higher than 3.2eV, the electron in valence band is excited by absorption of the energy, transferring to the conductive band. Then the electron-hole pair generated. Then the photogenerated electrons and holes are separated because of the self-field and the concentration diffusion. At this moment, the oxygen adsorbed on the surface of the nanoparticles trap the electrons, forming a superoxide anion. While the holes oxidize the hydroxide ions and water molecule adsorbed on the surface of the catalyst to hydroxyl radicals.

The main advantage of the chemiresistor based on MWCNT functionalized with MOX nanocryatals is the room temperature operation. The energy required for reactions are obtained from photon rather than the heat from high operating temperature.

In addition, the photocatalyst accelerate the reactions on the surface. Simultaneously, as a carrier of photocatalyst, MWCNT has large specific surface area and surface atomic ratio (about 50% of the total number of atoms), showing a special electronic effect and surface effects. When the gas passes through the carbon nanotubes, the diffusion rate is thousands of times than through the conventional catalyst particles. With the support of CNT, the activity and selectivity of the catalyst can be greatly improved. [4]

TiO2 and ZnO were employed as the photocatalysts deposited on Multi-walled CNT through Atomic Layer deposition.

2.3 Atomic Layer Deposition

Atomic Layer Deposition (ALD) is a precise method of deposition, offering control down to the atomic scale.

The principle of atomic layer deposition is similar to chemical vapor deposition (CVD) except the ALD reaction breaks the CVD reaction into two half-reactions, keeping the precursor materials separate during the reaction.

Figure 14 shows the principle of ALD. Before the deposition process, the substrate surface should have natural functionalization or be treated to functionalize the surface. This is accomplished through sequential pulsing of special precursor vapors, each of which forms about one atomic layer during each pulse (reaction cycle). Reaction cycles are then repeated until the desired film thickness is achieved, versus chemical vapor deposition that introduces multiple precursor materials simultaneously. [41]

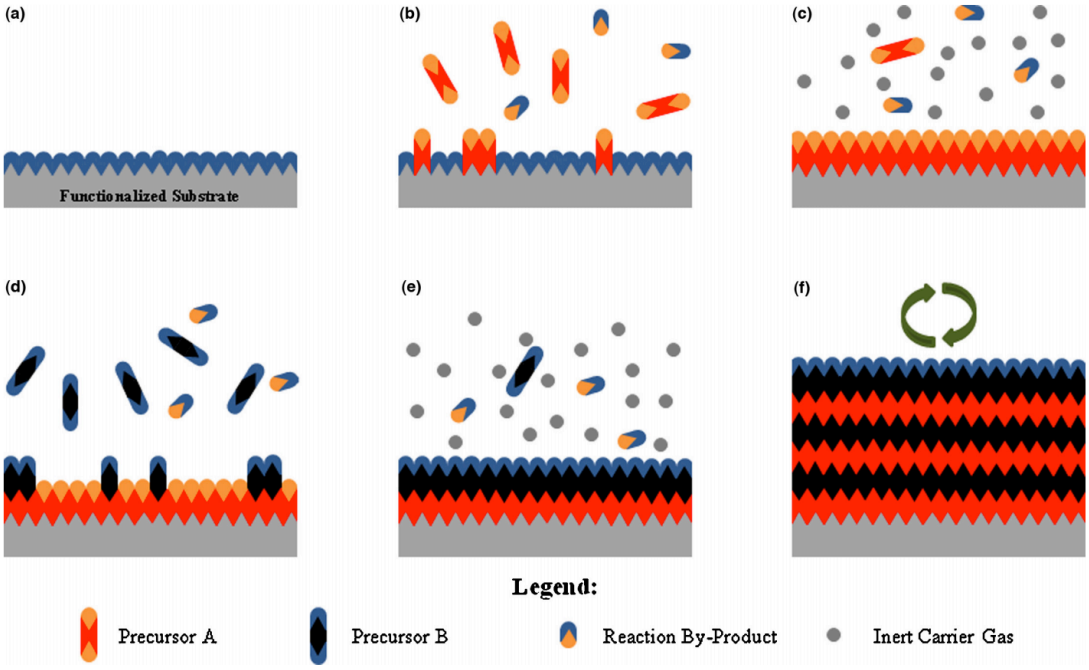

Figure 14 Different kinds of metrical deposited on functionalized surface of substrate

2.4 Humidity effects on sensors

There are various elements can affect the reaction on the active sensing layer of chemiresistor, including natural properties of base materials, surface areas and microstructure of sensing layers, surface additives, temperature and humidity, etc.[4] Humidity is one of the significant effects of metal oxide gas sensor, as many humidity sensors are based on metal oxide, indicating the humidity sensitive for metal oxide material. JJ Steele [42] fabricated nanostructured TiO2, SiO2 and Al2O3 thin film Glancing angle deposition (GLAD), which is sensitive for the humidity from 2% to 92%.

MWCNTs can also be employed as humidity sensing materials because of the hollow structure and the defects on the surface. L Liu et al. [43] deposited MWCNT networks between interdigitated electrodes (IDEs). The resistance of MWCNTs increases linearly with increasing the relative humidity from 25% to 95% RH with a sensitivity of 0.5%/%RH.

Therefore, for the hetero-structure chemiresistor gas sensor, environment humidity is a significant effect of the performance.

Chapter 3

Fabrication of MOX-MWCNT Sensors

3.1 Composite nanostructure of MOX/CNT gas sensor

The hydrocarbon gas sensor fabricated in this work is based on Multi-walled Carbon Nanotubes (MWCNT) functionalized with Metal Oxide (MOX) nanocrystals. The structure of the sensors are shown in Figure 15.

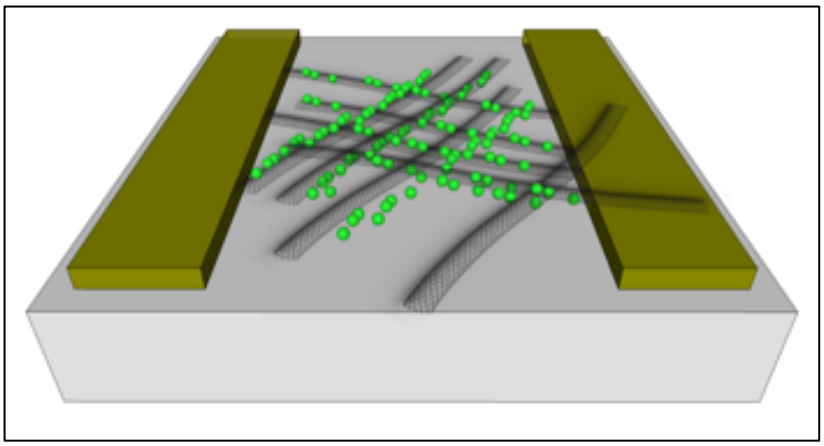

Figure 15 MOX deposited on the surface pretreated MWCNT

The Metal oxide nanoparticles were deposited on the surface of Multi-walled carbon nanotubes, which have been deposited between the gold electrodes and pretreated with oxygen plasma before deposition. ZnO and TiO_2 were employed as MOX in this study.

3.2 Fabrication Process

The fabrication of MOX-MWCNT is shown in Figure 16.

- ***Clean and dry:*** A 4" quartz wafer pretreated by Hexamethyldisilazane (HMDS) put into isopropyl solution was cleaned by ultrasonic for 5 minutes. Water in the air forming hydroxyl on the surface of wafer will affect the

adhesion between photoresist and substrate. Therefore, after drying the wafer by N_2, wafer should be heated in oven at 150°C for 25 minutes to remove the hydroxyl group. Wafer was cool down until it is ready for spinning resist.

- ***Coat:*** Wafer was held on a spinner chuck by vacuum and photoresist was coated to uniform thickness by spin coating. A bilayer of microchem lift-off resists 3A (LOR 3A) and S1813 photo resists was spin-coated on the wafer. The speed of spin coaster was set as 3000rpm for 35 seconds. [Figure 16. (b)]. Soft Bake took 1 minutes at 115°C (on hot plate) to evaporate the coating solvent and to increase the density of the resist after spin coating. Bake time and temperatures are dependent on the thickness of the photoresist film.

- ***Mask alignment and expose:*** Before the expose, mask alignment is very important. Glass mask was put on the holder of mask aligner and marks of left and right side of mask should be in one line. In this step, a direct laser writer (LW 405) was used to do the optical exposure. [Figure 16. (b)]

- ***Development:*** The wafer was soaked in developing solvent (solvent 315 and water mixed at ratio 3:1) for 30-35 seconds in order to remove exposed pattern of resist. [Figure 16. (c)] Wafer was cleaned in DI water and dried with a jet of nitrogen after developing. Since the duration of developing can severely affect the thickness of photoresist, wafer was investigated under microscopy after one cycle to ensure the resist removed perfectly.

- ***Metal deposition:*** A 100nm Au film on top of a 10nm Cr layer was deposited on the patterned photoresist using PVD 250 Lesker e-beam evaporator. [Figure 16. (d)]

- ***Photo-resist removal:*** Deposited metal was "lifted off" by ultrasonicating the samples immersed in an 1165 remover bath. [Figure 16. (e)]

- ***CNT deposition:*** A batch of 98% pure MWCNT with 12 nm average diameter, 10um average lengths, and a specific surface area of ~220 m^2/g was purchased from Sigma Aldrich. After dosing the wafer to chips with 4 sensors, the chips were place on the hot plate at 75°C. Using a microsyringe, the ultrasonicated solution of 1 mg/50 ml of MWCNT/ethanol was dropped to the area between electrodes, producing well dispersed CNT mesh. The heat on hoy plate can remove the solvent and improve the adhesion between MWCNT and substrate. [Fig. 16 (f)].

- ***O2 plasma treatment:*** The chips were treated by O_2 plasma for 10 seconds inside a reactive ion-etching chamber (March RIE) to prepare the surface of MWCNT before MOX deposition. [Fig. 16 (g)]

- ***Atomic Layer Deposition:*** Metal oxide nanoparticles were deposited on the MWCNT through ALD method. Diethylzinc (DEZ) and terakis (dimethylamino) titanium (TDMAT) was employed as precursor of ZnO nanoparticle deposition and TiO2 nanoparticle deposition respectively. The deposition process consists of 48 cycle and 217 cycles for ZnO and TiO2 nanoparticles respectively to obtain the thickness of MOX around 8nm. Both of two materials were performed at various temperature for from 175 to 225°C. As illustrated in ALD technology part, then MOX nanoparticle can only be deposited on the MWCNT with functionalized surface. [Fig. 16 (h)]

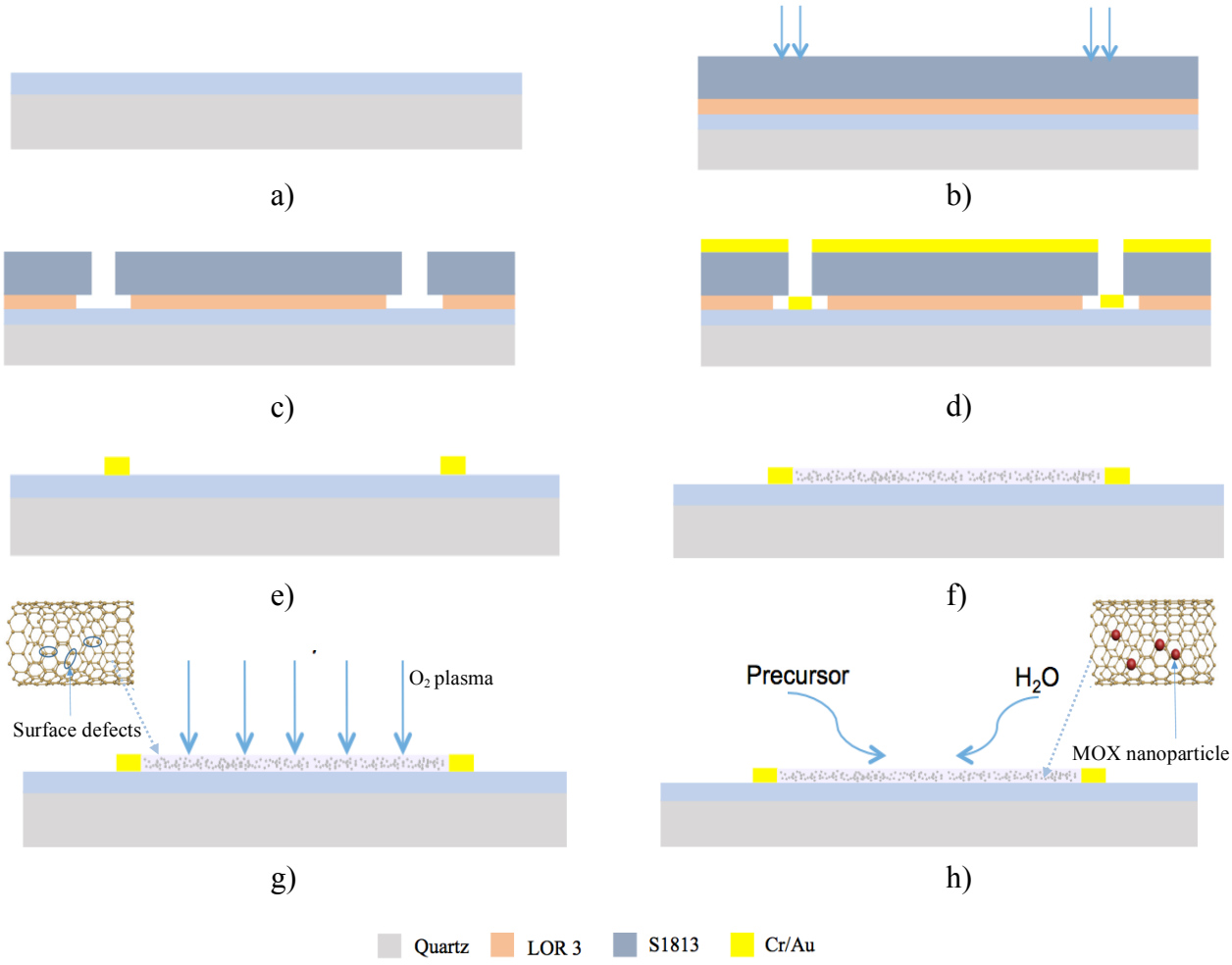

Figure 16 Fabrication processes of MOX-MWCNT sensor: a) Cleaned quartz wafer; b) Photoresist coated and directly laser writing; c) Development; d) Metal deposition; e) "lifted-off"; f) MWCNTs deposition; g) Oxygen plasma treatment; n) ALD deposition.

The fabricated and diced chip with sensors are shown in the figure x a). Figure x b) is the image of the sensor under x25 optical microscopy, illustrating the structure of the sensor.

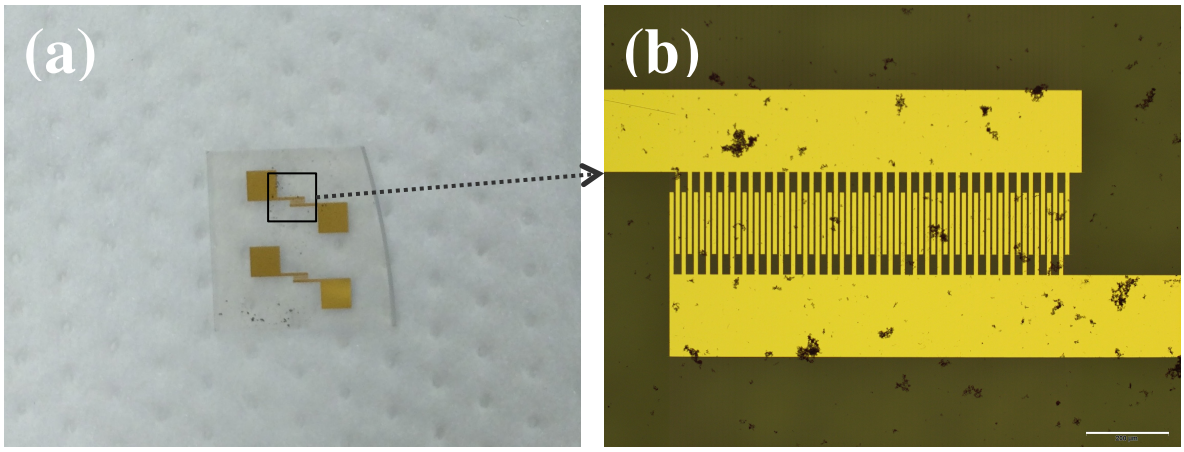

Figure 17 a) Fabricated gas sensor; b) optical microscopy image of gas sensor

Chapter 4

Test Methods

4.1 Different testing mode

As shown in Figure 18, a suitable voltage is applied to the MOX-MWCNT gas sensor. Measuring current through the sensor, the changes of resistance (sensor response) from air to the known amount of target gas can be recorded.

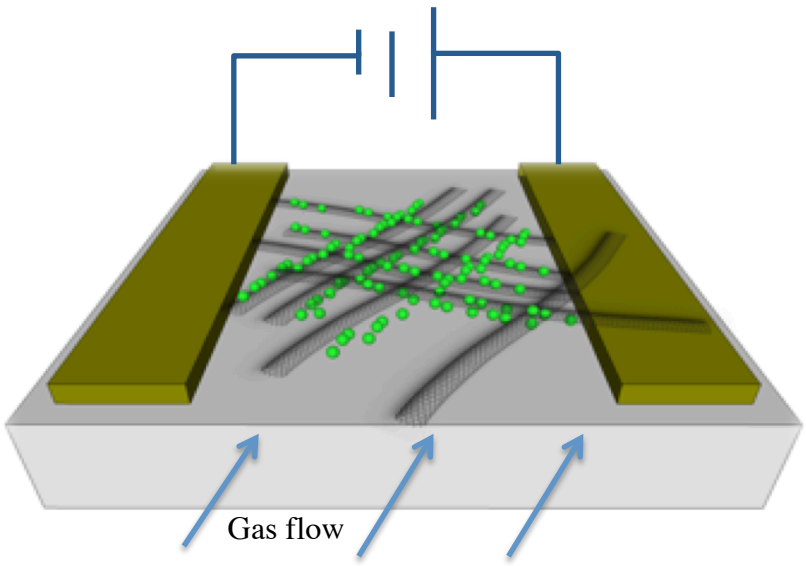

Figure 18 Electrical connection of gas sensor

There are two methods to measure the resistance [9]:

1) Flow- through method: The sensor is exposed under a continuous flow of a fixed amount of target gas, the concentration of which is controlled by the mixture of a carrier gas. With the Mass Flow Controller (MFC), the proportion of target gas in total amount can be controlled. The sensor response can be investigated as a function of different concentration.

2) Static environment method: The sensor is placed in an enclosed test chamber of a fixed volume. A fixed amount of gas is injected into the test chamber, mixing with the air in the chamber until the concentration of target gas reach

the desired one. The sensor response can be obtained as a function of time until the desired concentration reached.

In order to explore the performance of MOX-MWCNT chemiresistor sensors at higher humidity, sensors will be divided into two groups, which are supposed to be exposed under target gas at low humidity at 2% and high relative humidity at 50% respectively. By tracking and comparing the performance of a sensor continuously, aging effects can be investigated. Basic parameters characterizing sensor performance are analyzed.

The testing method employed in this work is based on the flow-through method. Sensors will be exposed under the analyzing gas at specific concentration for several circles in one test, which requires the easy operation to concentration changes.

4.2 Gas flow Setup

The schematic of test setup is shown in Figure 19. The wired MOX-MWCNT sensors placed in a sealed test chamber were connected to a Data acquisition (34972A LXI, Keysight, Inc.) pre-connected with a DC power supply (Model 1693, BK Precision). Dry N_2 and synthetic air (20.8% O_2, N_2 balance) were use as carrier gas for VOCs (Toluene and Benzene) and CH4 respectively to purge the target gas from test chamber after each cycle of exposure under target gas. They are introduced to the test chamber at constant flow rate (2 SLPM), which can be controlled by mass flow controller (MFC). Transferring the output signal from data acquisition to the computer, sensor responses can be recorded.

For the experiments run at high humidity level (50% relative humidity), target gas went through the bubbler filled with water before introduced to the test chamber to get higher humidity. The bubbler was place on a hot plat at 85C. The humidity obtained form this condition was 50%± 2%. Carrier gas line connected to the bubbler as well to keep the constant relative humidity inside the chamber. Benzene and N2 in figure x are employed as example to show the gas flow in high RH experiment.

Toluene and N_2 gas in figure x are employed to illustrate how the experiment operated at low RH level. Since there is only one test chamber in the system, when experiment is run at low RH level, the high RH line should be removed from the system and vice versa.

During the experiment, the relative humidity (RH) and temperature inside the test chamber were continuously monitored and recorded by the data-logger (34972A LXI, Keysight, Inc.).

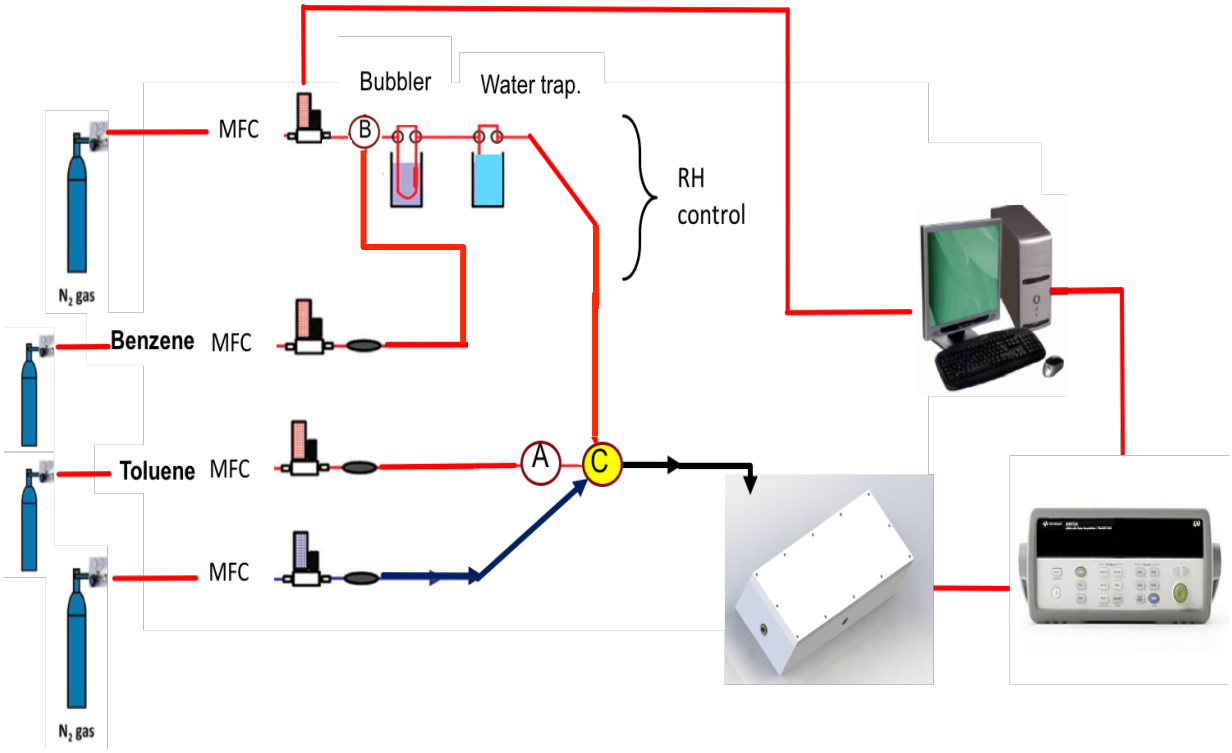

Figure 19 Schematic of gas flow for MOX-MWCNT at 2% RH experiment and 50% RH experiment.

4.3 Parameters for target gas exposure

To investigate the response time and recovery time, sensors were exposed under target gas for several cycles in one experiment.[Figure 20] Before the first injection of target gas, carrier gas was introduced to the test chamber to purge the room air and remove the moisture or bring moisture in the chamber, ensuring no effects from other hydrocarbons in the air and keeping stable RH level inside the chamber before several cycles of target gas exposure. The time for carrier gas injection before 10-20 minutes exposure under target gas is 60 minutes in this work.

Sensors fabricated with different metal oxides under different temperatures were tested under three different target gases respectively. The target gas sources are mixture of 10ppm methane in dry synthetic air (20.8% O_2, N_2 balance), mixture of 10ppm toluene in dry nitrogen and mixture of 50ppm benzene in dry nitrogen (Praxair, Inc.). Table 3. illustrates the parameters for experiments at both of low and high RH level.

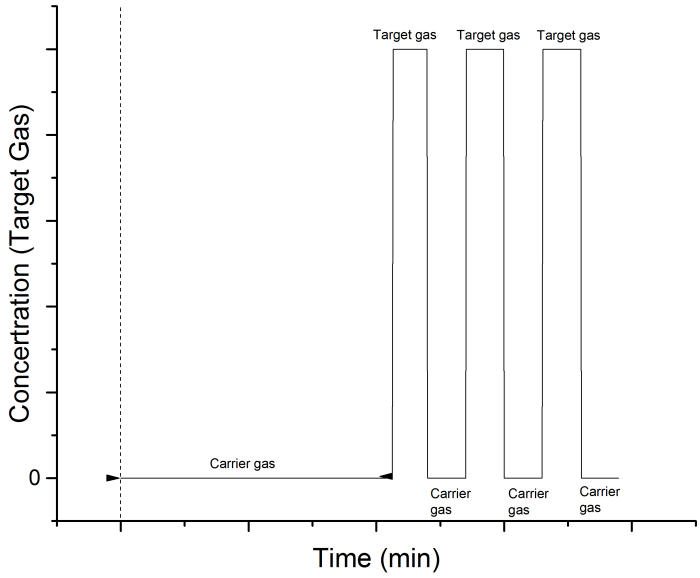

Figure 20 Operating mode of carrier gas and target gas

Table 3 Parameters set for different sensors

Sensors	*Target gas*	*Concentration (ppm)*	*Carrier gas*	*Exposure time (min)*	*Storage*
Experiment at low RH level (2%)					
ZnO-MWCNT-175 °C	Methane	10	20.8% O_2	10	Room air
	Benzene	50	N_2	20	
	Toluene	10	N_2	20	
ZnO-MWCNT-200 °C	Methane	10	20.8% O_2	10	
	Benzene	50	N_2	20	
	Toluene	10	N_2	20	
ZnO-MWCNT-220 °C	Methane	10	20.8% O_2	10	
	Benzene	50	N_2	20	
	Toluene	10	N_2	20	
TiO2-MWCNT-175°C	Methane	10	20.8% O_2	10	Room temperature
	Benzene	50	N_2	20	
	Toluene	10	N_2	20	
TiO2-MWCNT-200°C	Methane	10	20.8% O_2	10	
	Benzene	50	N_2	20	
	Toluene	10	N_2	20	
TiO2-MWCNT-225°C	Methane	10	20.8% O_2	10	
	Benzene	50	N_2	20	
	Toluene	10	N_2	20	
Experiment at high RH level (50%)					

ZnO-MWCNT-175 °C	Methane	10	20.8% O_2	10	50% RH Room temperature
	Benzene	50	N_2	20	
	Toluene	10	N_2	20	

Sensitivity and selectivity of the sensors (mentioned in as characteristics of chemiresistor) listed in the table were investigated. To investigate the aging effects of specific MOX-MWCNT sensor, ZnO-MWCNT sensor (ALD at 175°C) was chosen to be recorded the performance under methane every 3 or 4 days.

4.4 Electrical testing process

1) Electrical connection

The soldered sensors (Fig 21. a) placed in the sealed test chamber (Fig 21.b) were connected to the data acquisition (34972A LXI, Keysight, Inc.) pre-connected with a DC power supply (Model 1693, BK Precision). Voltage was applied to sensors. Resistances of sensors can be read from the data acquisition.
Connect the Mass flow controller to the charger.

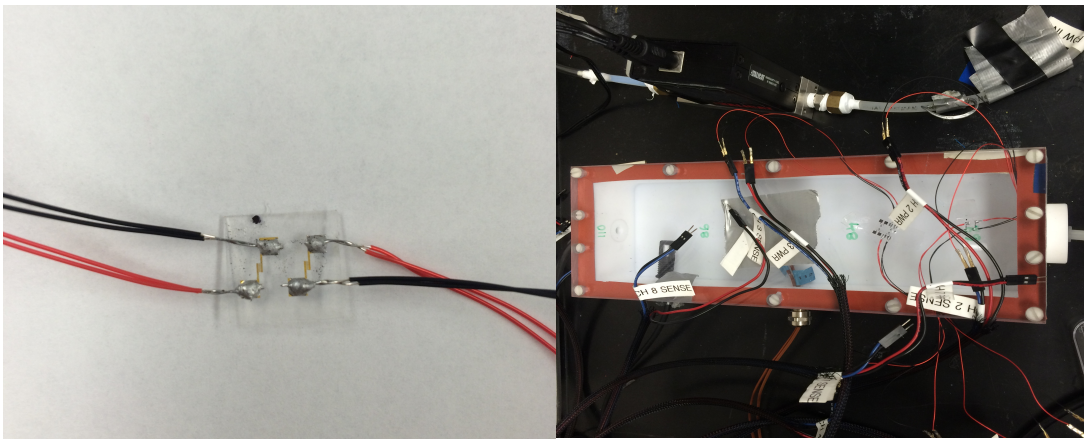

a) b)

Figure 21 a) Wired gas sensor; b) electrical connection between data acquisition and sensors in test chamber

2) Open the tank of carrier gas and target gas

The maximum flow rate automatically set for mass flow controller is 0 every time when the MFC is switched on. Therefore, gases from tanks will not enter the test chamber before testing.

3) Start the LabView

The mass flow rates for carrier gas and target were set by computer, according to the order shown in figure x.

Simultaneously, the resistances of sensors under gases were recorded by computer.

4) End the test

Close the gas tank and switch off MFC. Disconnect sensors and data acquisition. Sensors were not removed from test chamber, which was connected to room air after test. The data acquisition kept tracking the temperature and humidity in the test chamber during the storage of sensors.

Chapter 5

Results

5.1 Nanoparticles deposition on MWCNT

In the fabrication process about MWCNT deposition, the MWCNT solution was dropped to the substrate through micro-syringe by hand. The volume of droplets and the distribution of MWCNT are various for each sensor. Therefore, the resistances of sensors were different, varying from 100Ω to 1MΩ. Before the electrical test, TEM grids fabricated with the same conditions as sensors were investigated through Transmission/Scanning Electrical Microscopy (T/SEM). As shown in the TEM image in Figure 22 (d), the MWCNT meshes were deposited between Au electrodes. Figure. 22 (e) illustrate the growth mechanism of ZnO. [44].

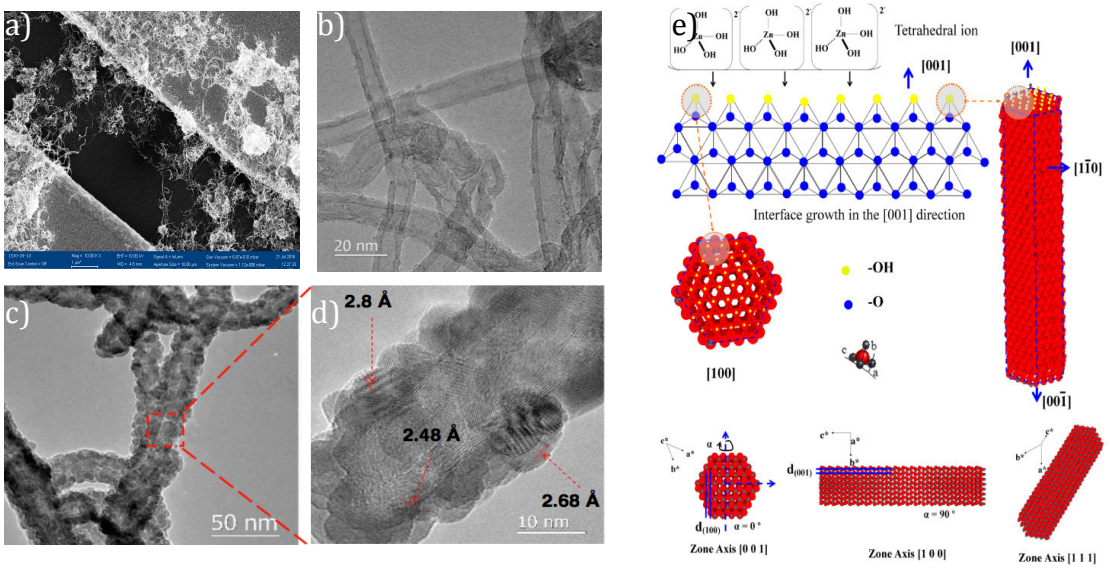

Figure 22 a) SEM image of MWCNT between Au; b) TEM images of MWCNT; c) TEM image of MWCNTs after ALD; d) high resolution of TEM image; e) Growth mechanism of ZnO crystal.

There are three direction of the ZnO crystal growth. In the [001] direction, the ZnO Nano-crystalline presents nearly ideal hexagon since the ratio of lattice constant c/a is 1.6 (~1.633). The high resolution TEM image of ZnO-MWCNT (ALD at 175 C) sample in Figure 22 d) shows interplanar spacing of 2.8Å, 2.68Å and 2.48Å corresponding to <100>, <002> and <101> planes of ZnO respectively. Therefore, the ZnO nanoparticles were deposited successfully on MWCNT by ALD. As mentioned in the introduction of ALD technology, only the functionalized substrate surface enables the reaction with precursor. In this work, only MWCNT are treated with O2 plasma to get the deposition of ZnO nanocrystals.

5.2 Gas sensing properties

5.2.1 Sensing properties at RH 2%

Following the experiment processes, the sensor responses of ZnO-MWCNT chemiresistive gas sensors were obtained. Figure 23(a) (b) (d) represent the response of multiple sensors (ZnO-MWCNT deposited at 175 °C) under 10ppm CH4, 10ppm toluene and 50ppm benzene respectively. Sensor response is a function between resistance changes and gas concentration. The multiple sensors in the same experiment responded to the same target gas and recovered in the carrier gas almost simultaneously, indicating the reliable and repeatable of the sensors response experiment.

The sensitivities of ZnO-MWCNT (ALD 175 °C) working in different target gases are outlined in Figure 23(c).

The sensitivities of sensors can be defined in different ways. The definition employed in this work is the ratio of the resistance difference to the resistance in air. Therefore, the sensitivities of ZnO – MWCNT sensors for CH_4, Toluene and Benzene can be calculated following the equation:

$$S(\%) = \frac{R_0 - R_s}{R_0} * 100$$

Where R_0 is the baseline resistance and the R_s is the resistance under target gas.

Standard deviation is also employed to represent the stability of sensors, which can be calculated by the equation:

$$\sigma = \sqrt{\frac{1}{N}\sum_{i=1}^{N}(x_I - \mu)^2}$$

The sensitivity of ZnO-MWCNT hydrocarbon gas senor (ALD 175°C) under 10ppm methane and toluene are 0.11451% ± 0.01057%, and 0.14024% ±0.01001%

respectively. While the sensitivity under 50ppm benzene is 0.14024%± 0.03872%. ZnO-MWCNT (ALD 175°C) hydrocarbon gas senor is more sensitive to methane than toluene at the same concentration. The sensitivities of ZnO-MWCNT hydrocarbon gas sensor under those three gases are shown in Figure 23 (c).

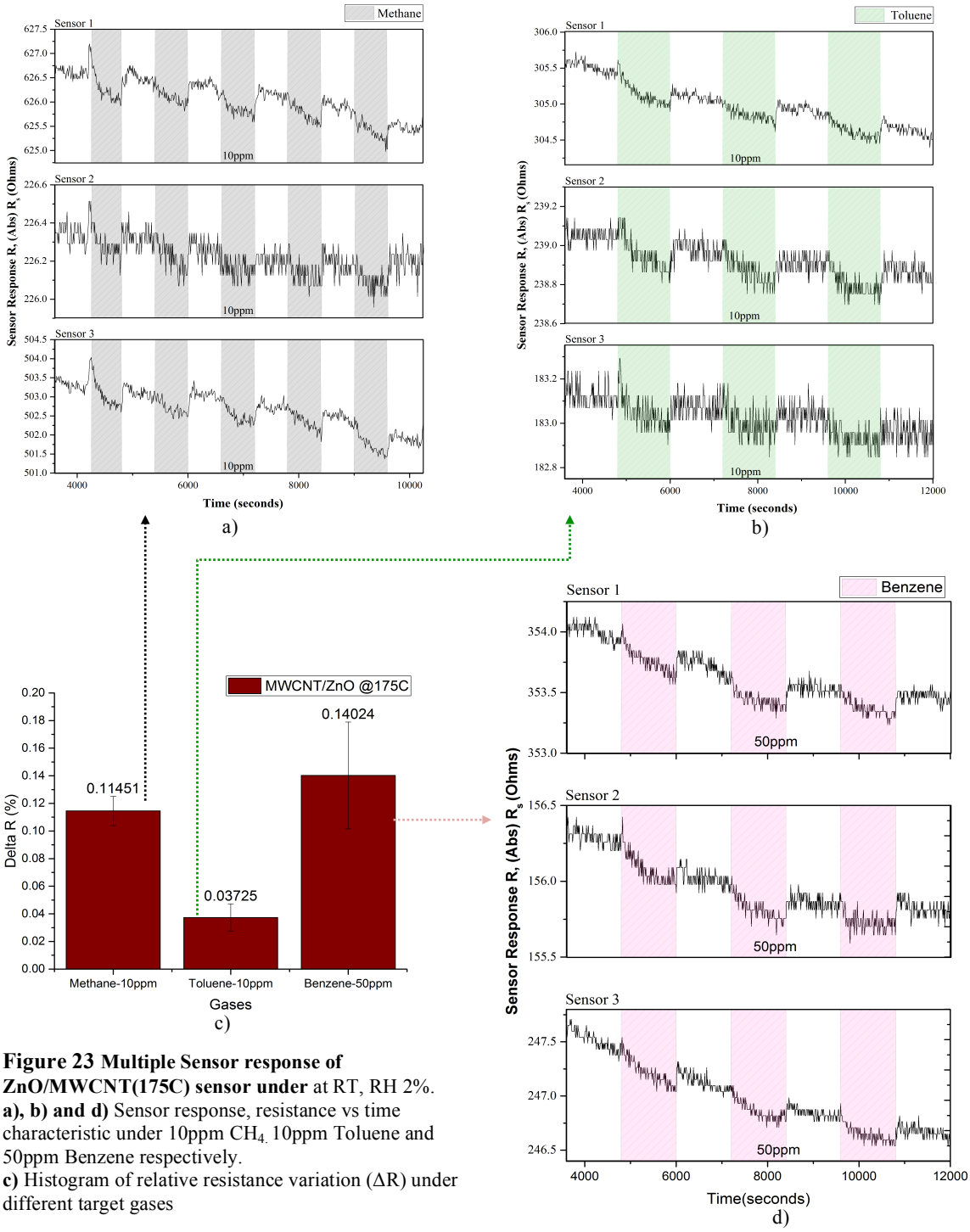

Figure 23 Multiple Sensor response of ZnO/MWCNT(175C) sensor under at RT, RH 2%.
a), b) and d) Sensor response, resistance vs time characteristic under 10ppm CH_4, 10ppm Toluene and 50ppm Benzene respectively.
c) Histogram of relative resistance variation (ΔR) under different target gases

The ZnO-MWCNT fabricated at different ALD temperature 200°C and 220°C were tested at the same conditions as ZnO-MWCNT (ALD 175°C). [same concentration of The sensor responses of those sensors under CH_4, toluene and benzene are at room temperature and 2% relative humidity are shown in Figure 24 and Figure 25 respectively.

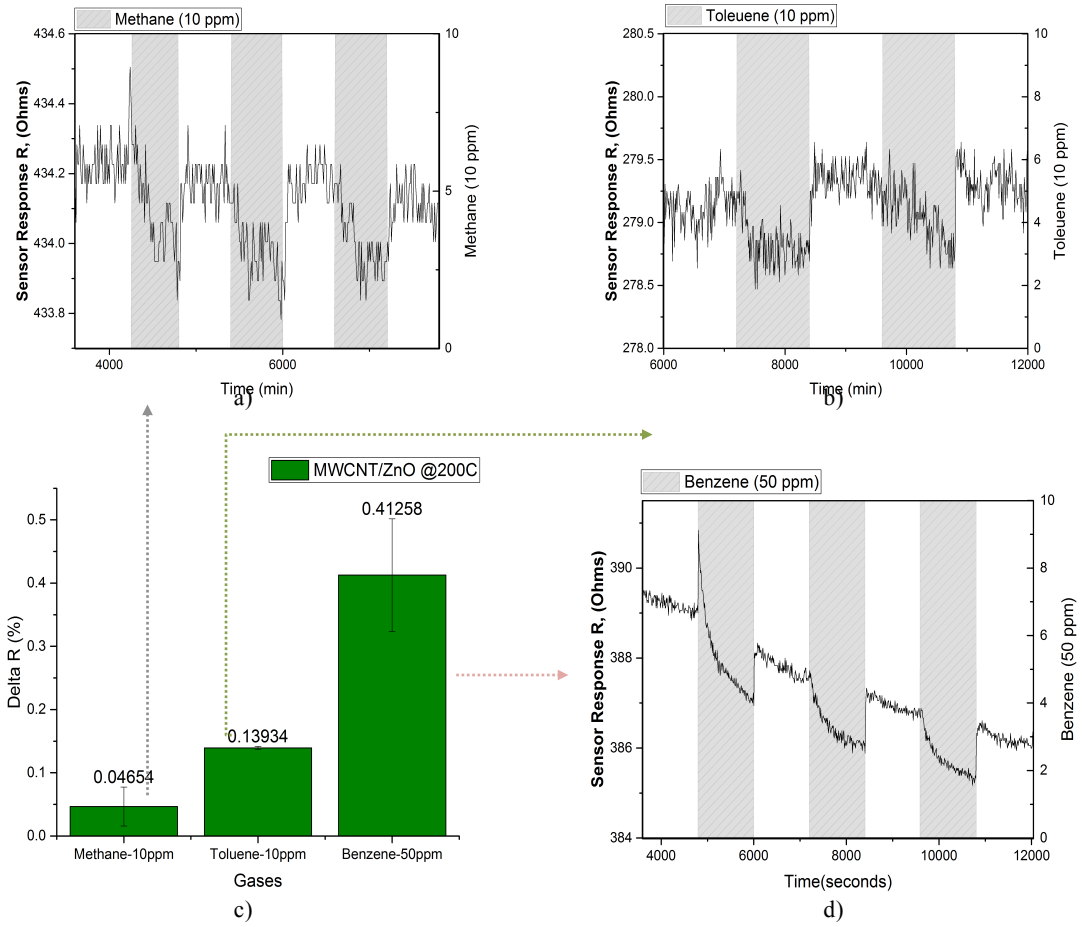

Figure 24 Sensor response of ZnO/MWCNT(200C) sensor under at RT, RH 2%.
a), b) and d) Sensor response, resistance vs time characteristic under 10ppm CH_4. 10ppm Toluene and 50ppm Benzene respectively.
c) Histogram of relative resistance variation (ΔR) under different target gases

Sensitivities of ZnO- MWCNTs (ALD 200°C) hydrocarbon gas sensor under 10ppm methane and 10ppm toluene are 0.04654% ± 0.03084% and 0.13934% ± 0.00253% respectively, indicating the ZnO- MWCNT (ALD 200°C) hydrocarbon gas sensor is more sensitive to toluene comparing with the same concentration methane. The sensitivity under 50ppm benzene for this sensor is 0.41258% ± 0.08902%, which is almost 3 times of the sensitivity of ZnO-MWCNT (ALD 175°C) gas.

Similarly, the sensitivities of ZnO-MWCNT (ALD 220°C) hydrocarbon gas sensor under methane and toluene at the same concentration (10ppm) are 0.14906% ± 0.01994% and 0.25264% ± 0.05224%. And the sensitivity under 50ppm benzene is 0.23708% ± 0.05933%, which is less than the sensitivity under toluene.

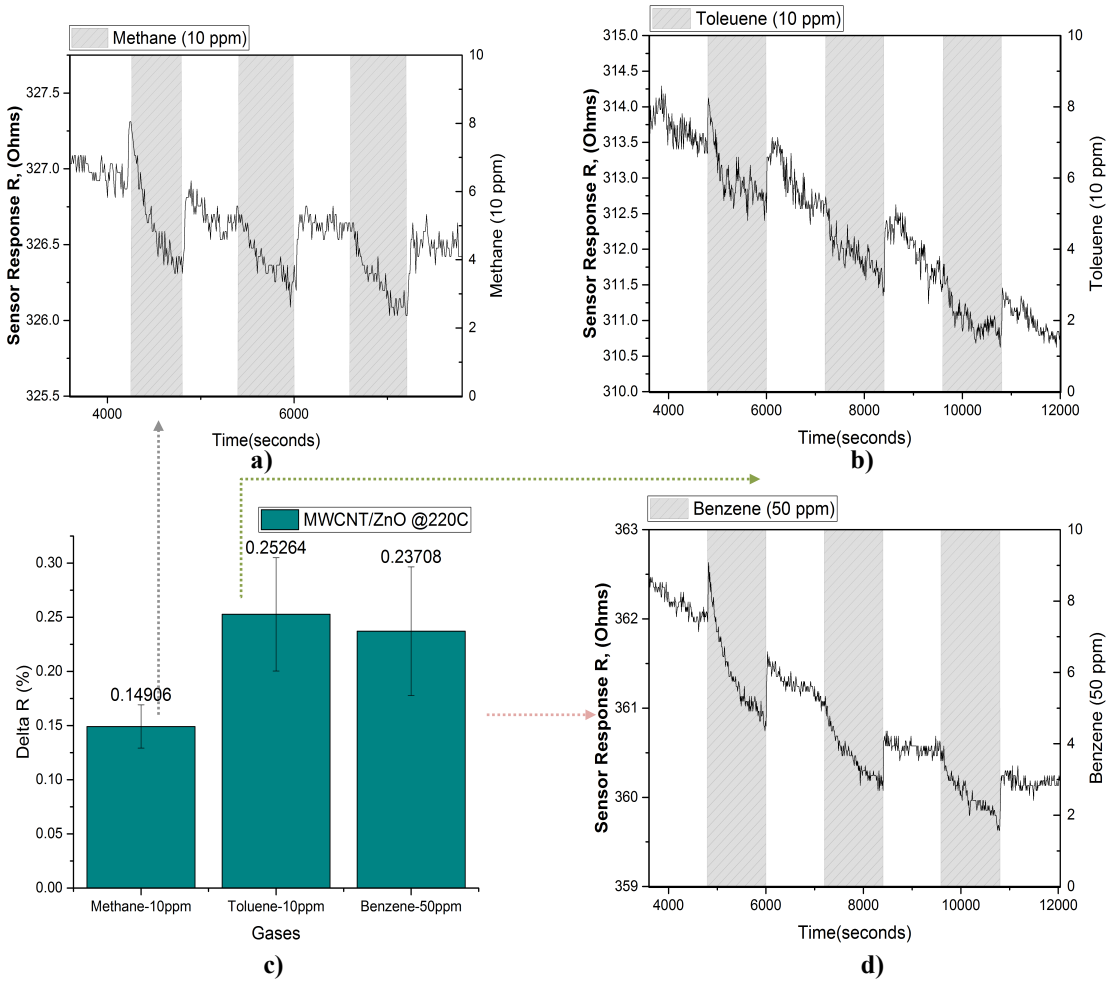

Figure 25 **Sensor response of ZnO/MWCNT(220 C) sensor under** at RT, RH 2%.
a), b) and d) Sensor response, resistance vs time characteristic under 10ppm CH_4, 10ppm Toluene and 50ppm Benzene respectively.
c) Histogram of relative resistance variation (ΔR) under different target gases.

Since methane is our main target gas, the sensitivities of the ZnO-MWCNTs fabricated under different temperatures under methane are compared. The sensitivity of ZnO-MWCNT (175 °C) and ZnO-MWCNTs (220 °C) are higher than that of ZnO-MWCNTs. The sensitivity of ZnO- MWCNT sensor (175°C) under methane is ~3 times of that under toluene, while the sensitivity of ZnO-MWCNT gas sensor (220°C) under toluene is less than 2 times of that under methane. Although the ZnO-MWCNT (220) is a bit more sensitive to methane, ZnO- MWCNT (175°C) is employed in aging test because of the better selectivity between methane and toluene.

As important characteristics, response time and recovery time is investigated. The response time of the sensor is commonly specified by the T90, which is illustrated in the chapter 2. The signal of sensor response is smoothed by percentile filter with 5 points of window. (Figure 26). Target gas was injected at point A and purged at point B. The Y-axis values of point A and B (5408.68099 Ω and

502.59297Ω) are the baseline resistance and the final resistance under methane of the sensor ZnO- MWCNT (175°C) respectively.

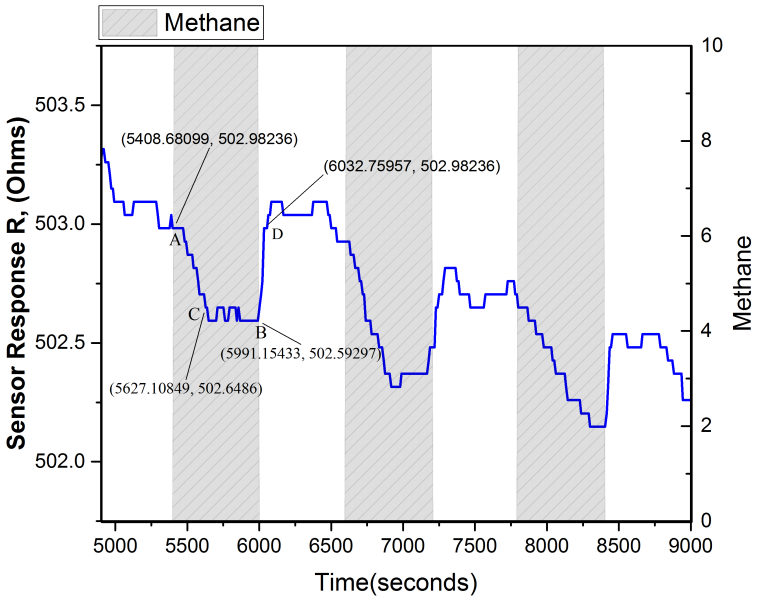

Figure 26 Sensor response under 10ppm methane at RT, 2%RH

The 90% value of final resistance can be calculated as following:

$$R_{90} = R_0 + 0.9 * (R_S - R_0)$$

Where R_0 is the baseline value and R_s is the final resistance under target gas. According to the calculation, the point C can be found in the curve and time between point A and point C implies the response time of the sensor.

Similarly, the Y-axis value of point D is equal to the baseline resistance, indicating the sensor recovers from target gas at this point. The time between point B and C is the recovery time of ZnO-MWCNT (ALD 175°C) gas sensor. Response time and recovery time under CH4, toluene and benzene are outlined in table x.

Target Gas	***Response time (s)***	***Recovery time (s)***
Methane	225.46 ± 26.42	65.87 ± 4.90
Toluene	325.88 ± 21.37	121.47 ± 5.0
Benzene	260.03 ± 29.42	69.34 ± 9.81

Comparing the response time and recovery time under each target gas. The sensor has relatively fast response and quick recovery for Methane. In general, the response time is longer than recovery time for each target gas.

5.2.2 Aging effects of ZnO-MWCNT (ALD 175℃)

ZnO-MWCNT gas sensors suppose to be operated at common condition. Therefore, two ZnO-MWCNT (ALD 175°C) sensors were stored at RT (22 °C) and room RH (35%±5%). The sensor responses under methane at 2% RH were recorded immediately after fabrication [Figure 27 (a)]. After 30 days storage in room RH at RT, the performance of sensors was recorded again [Figure (b)].

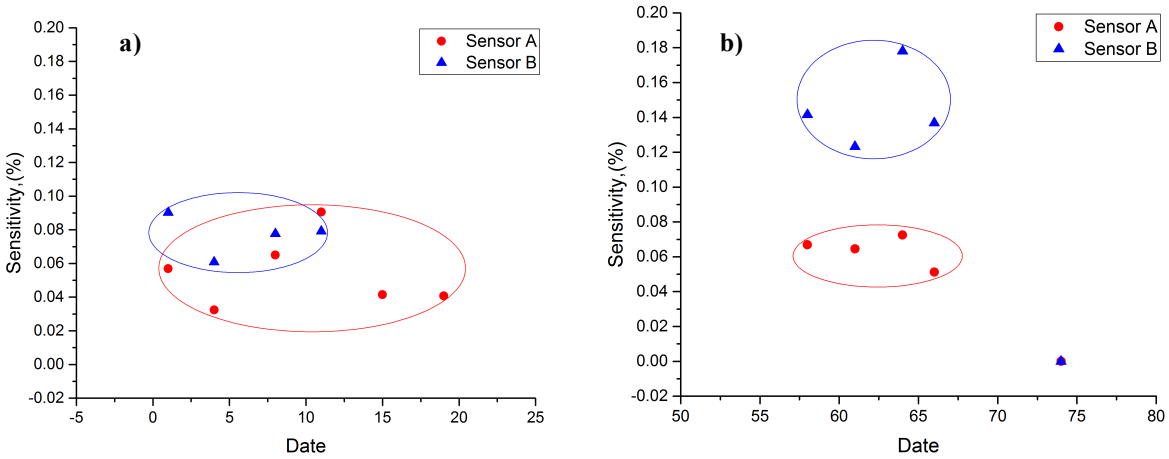

Figure 27 **a)** Relative Resistance variation (ΔR) as a function of date for ZnO/MWCNT(175C) sensor [from first exposure]
b) Relative Resistance variation (ΔR) as a function of date for ZnO/MWCNT(175C) sensor [Tested after 1 month storage]

Relative resistance variation (sensitivity) of sensor A was stable during 70 days after fabrication, while the sensitivity of sensor B increased after storage. After 74 days aging in room RH at RT. Both the sensor A and B had no capability of sensing the methane. The sensor response (resistance change) of sensor A exposed under methane 60 days after fabrication is shown in figure x. Comparing with the first exposure under methane right after fabrication (Figure a)), the baseline value increased from 226.19Ω to 449.75 Ω where the sensor was aged for 60 days in common conditions.

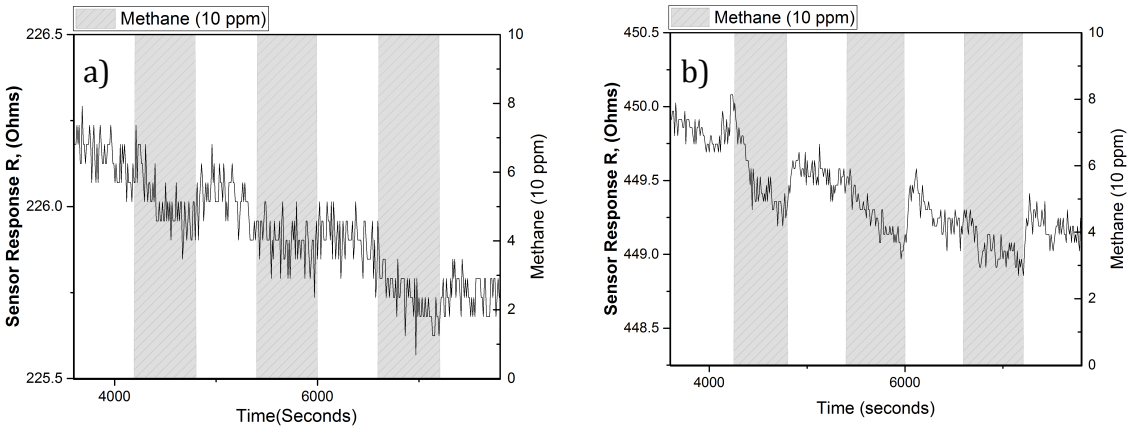

Figure 28 a) Sensor response of Sensor A without aging; b) Sensor response of Sensor A after 60 days aging in RT, room RH

shown in Figure 29 (a). The resistance dramatically increased to 100kΩ. Another sensor C fabricated 43 days later than sensors A, was tested in the same experiment with sensor A [Figure 29(b)]. Sensor C was place in the same storage chamber with sensor A after fabrication.

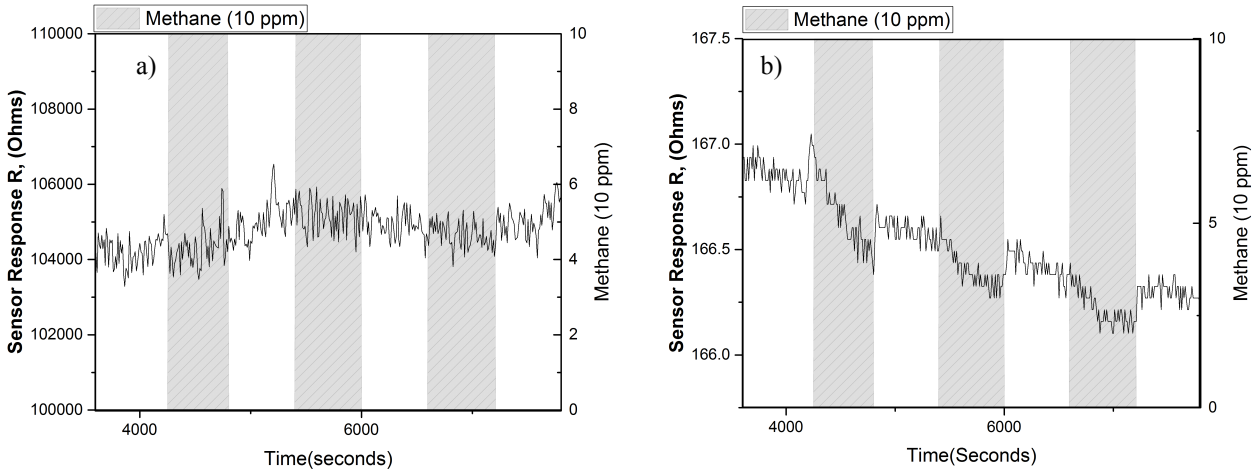

Figure 29 a) Sensor response of Sensor A after 74 days aging at RT, room RH. b) Sensor response of Sensor C after 30 days aging at RT, room RH.

5.2.3 Sensing properties at RH 50%

Respectively, ZnO-MWCNT gas sensor D, E and F, a group of sensors stored at RT, 50% RH, were tested under CH4, toluene and benzene at RT, 50% RH. The sensor responses are shown in Figure 30, representing no sensitivity under any of three gas at RT, 50% RH.

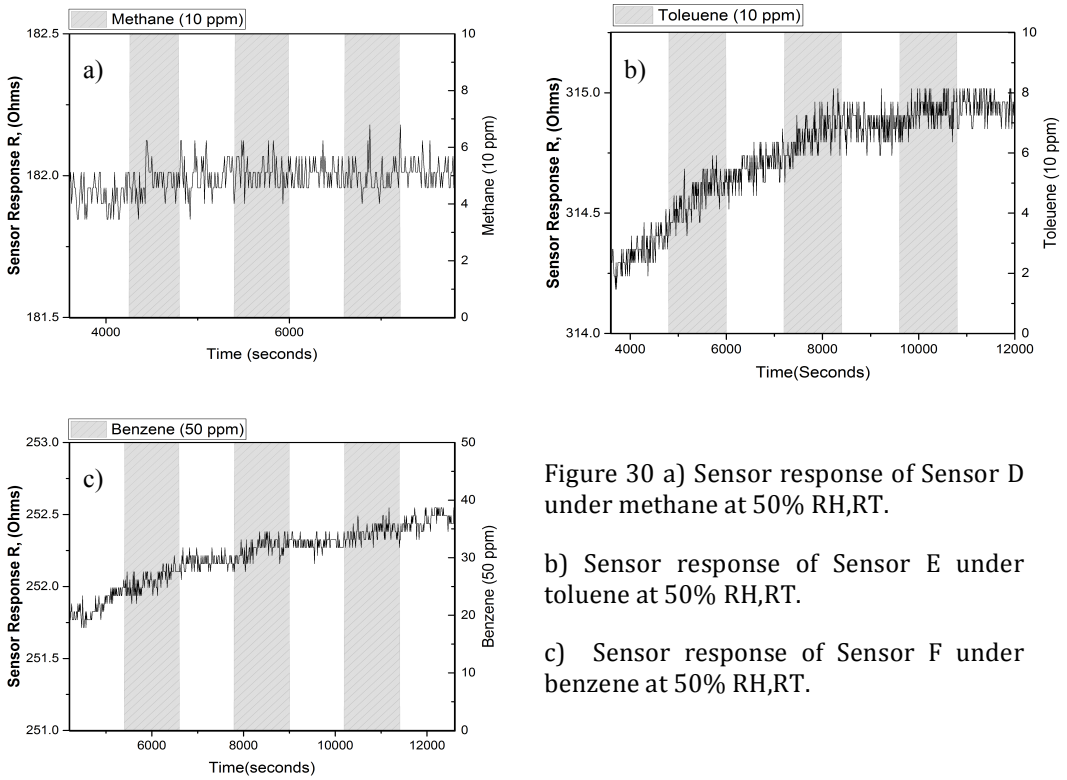

Figure 30 a) Sensor response of Sensor D under methane at 50% RH,RT.

b) Sensor response of Sensor E under toluene at 50% RH,RT.

c) Sensor response of Sensor F under benzene at 50% RH,RT.

5.2.4 Characteristics of TiO2-MWCNT gas sensor

In this work, TiO2-MWCNT gas sensor were fabricated and tested under CH4, toluene and benzene at RT and 2% RH as well to explore the different catalyst effect of different metal oxide nanoparticles. The sensitivities are calculated similarly with that of ZnO-MWCNT gas sensor, which are listed in Table 4.

Table 4 Sensitivity of TiO2-MWCNT (ALD 175C) gas sensor under 3 gases

Sensors	***Target gas***	***Sensitivity***
TiO2-MWCNT (ALD 175C)	Methane	0.31121%±0.01628%
	Toluene	0.15085%±0.02502%
	Benzene	0.08606%±0.02898%
TiO2-MWCNT (ALD 200C)	Methane	0.24259%±0.04362%
	Toluene	0.0312%±0.0281%
	Benzene	0.01618%±0.03967%
TiO2-MWCNT (ALD 225C)	Methane	0.08606%±0.00856%
	Toluene	0.05573%±0.02560%
	Benzene	0.07747%±0.06511%

Chapter 6

Discussion

6.1 mechanism of ZnO - MWCNT

This hetero-structure chemiresistor was operated at room temperature. Nano-scaled ZnO was used as a photon catalyst, which can absorb the sunlight across the ultraviolet–visible (UV–vis) region to produce electrons and holes. The energy from sunlight First step of target gas activation on oxide material is the reaction with surface Oxygen radical. Methane is used to illustrate the mechanism [45]:

$$\text{Oxide} - \text{O}^{\cdot} + \text{CH}_4 \rightarrow \ {}^{\cdot}\text{CH}_3 + \text{HO} - \text{oxide} \quad (1)$$

When the nanoscaled ZnO is illuminated under light, the surface electron and hole are generated

$$\text{ZnO} \rightarrow \text{Zn}^{\cdot}\text{O} + \text{e}^{-} \ (hv \text{ absorbed}) \quad (2)$$

The generated electron and hole will attract the atom H from CH4 molecule

$$\text{Zn}^{\cdot}\text{O} + \ \text{CH}_4 \rightarrow \text{ZnOH} + \text{CH}_3^{\cdot} \quad (3)$$
$$\text{O}_2 \rightarrow \text{O}_2^{-} \ (hv \text{ absorbed}) \quad (4)$$

The generation of superoxide anion radicals will initiate further oxidation of the methyl radicals:

$${}^{\cdot}\text{CH}_3 + \text{O}_2^{-} \rightarrow \text{CH}_2\text{O} + \text{OH}^{-} \quad (5)$$
$$\text{OH}^{-} + \text{ZnOH} \rightarrow \text{ZnO} + \text{H}_2\text{O} \quad (6)$$

After the ZnOH Oxidized to ZnO, the reaction start from (2), building a cycle among the above reactions. Figurex shows the reaction chain.

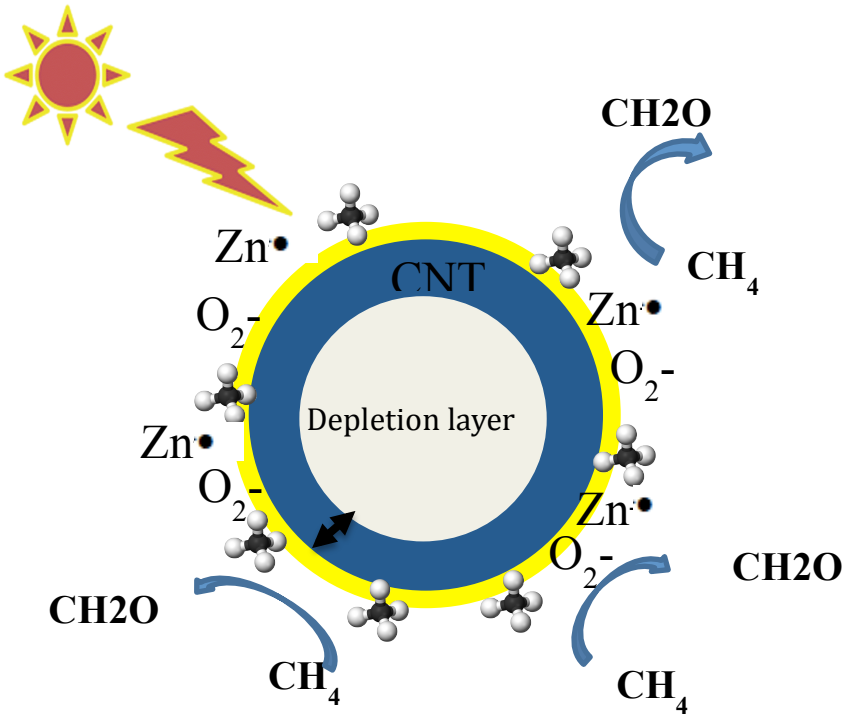

Figure 31 Reaction chain on the surface of ZnO nanoparticle

The light and the oxygen are introduced from the outside of the cycle, which are critical for ZnO-MWCNT sensing. Therefore, synthetic air with 20.8% O_2 were employed as the carrier gas for methane. Another vital element is the separation of the electrons and holes in space to avoid the recombination. As electron sink, MWCNT can exact the electron / pair holes to prevent the recombination on the surface of ZnO.[46]

When the sensor is illuminated under light in air, oxygen molecules are adsorbed on the surface of ZnO nanoparticles and extract electrons from the conduction band forming oxygen species [shown in reaction (4)]. Consequently, a depletion layer is built on the surface of ZnO nanoparticles, increasing the resistance of the sensor. Once the methane molecules are absorbed on the ZnO surface, reactions (3)-(6) occurs on the surface, freeing the electrons on ZnO. Therefore, the conductivity of ZnO increases under the exposure under methane, meaning resistance decreases during exposure. The resistance change under toluene and benzene are similar with methane, interacting with oxygen ions and enabling the electrons come back to conductive band. All the figures showing resistance change in results confirm this mechanism.

In the idea case, after 60 minutes injection of carrier gas, sensors are exposed under methane and carrier gas for 10 minutes respectively in one cycle. For toluene, the exposure time is increased to 20 minutes in that the response time of toluene (in Table 4) is more than a half of the 10 minutes. The carrier gas will purge the target gas

molecules inside the chamber before next cycle. However, the target molecules cannot be removed completely. The water molecules produced from the reaction chain shown in reaction (6) have the opportunity to react with the oxygen ion on the surface of ZnO, leading the decrease of electrical resistance. Therefore, the baseline value cannot be recovered to the pervious value.

6.2 Humidity effect on ZnO-MWCNT gas sensor

Form Figure 30, there were no responses of the sensor under CH4, toluene or benzene, which means there was no interaction with target gas molecules on the surface. Gas molecules cannot react with the oxygen ions on the surface of ZnO. In this experiment, the only different condition with the experiment run at 2% relative humidity is the introduction of more water molecules. As shown in Figure 32, water molecules can react with negative charged oxygen ions on the surface, forming less reactive hydroxyl groups, potentially inhibiting the gas sensing reaction. The water molecules physically absorbed on the surface of ZnO will decrease surface area for sensing as well. Since the carrier gas with 50% RH was injected into the test chamber 60 minutes earlier than target gas, the hydroxyl group was formed before the reaction of target gas. The resistance under exposure of target gas will not changed in that there is no change of electrical structure during exposure.

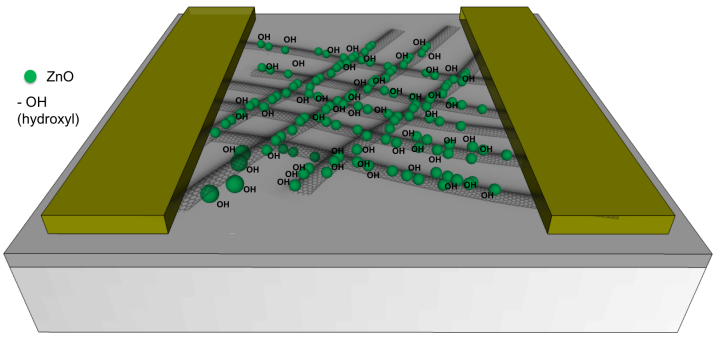

Figure 32 Hydroxyl groups form on the surface of ZnO

To explore the humidity effect on the ZnO- MWCNT gas sensor, one more test for Sensor D was designed. After the test at 50% RH, the sensor stored in 50%RH was tested under the same conditions expect for the RH level. The sensor response was shown in figure x. Comparing with the performance under 50% RH, sensor D has high sensitivity for methane at 2% RH.

Although there was no response at 50% RH, The sensor still have sensitivity to methane when it was put at 2% RH. That indicates the adsorption of water on the surface of ZnO –MWCNT materials is reversible.

The baseline value of sensor at 50%RH (181.13 Ω) in Figure x is higher than the value at 2% RH (177.66 Ω) in Figure 33. For ZnO nanocrystals, water molecule in air can form hydroxyl group on the surface, resulting in the decrease of electrical resistance at 50% RH. However, MWCNT absorbed the water molecules from ambient environment as well, resulting the increase of the baseline resistance. The hydrogen in absorbed water molecule can form a weak bond with one of the surface C atoms on MWCNTs. [x]. The electrons from adsorbed water molecules transfer to the valence band, decreasing the number of holes and resulting in increase of the electrical resistance.

The calculated sensitivity (0.20386%±0.076292%) is almost 2 times of average of sensitivity for sensors stored at room RH, indicating suitable humidity treatment may improve the performance of sensor, which is confirmed by the sensor B in Figure 27 b).

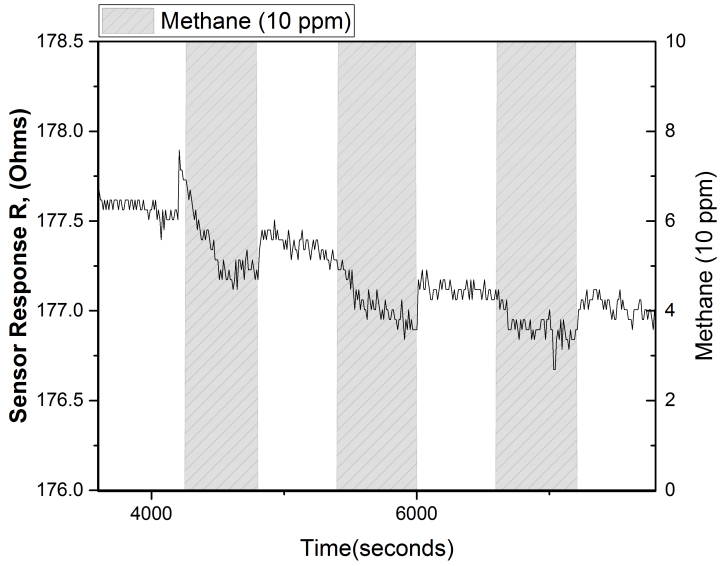

Figure 33 Sensor response of Sensor D exposed under 10ppm methane at 2% RH,RT

6.3 Aging effects on ZnO-MWCNT (ALD 175C)

In this work, the sensors were aged at RT and room RH. As illustrated in humidity effect, water molecules in the air will be absorbed by both of ZnO and MWCNT during the storage. After the absorption, the conductivity of ZnO will increase due to the freed electrons transferring to conductive band, resulting in the decrease of resistance. On the contrary, the resistance of MWCNT will decrease because of the decrease of the holes. Since the baseline value of aged sensor A in Figure x is higher than the value before aging, water absorption of MWCNT dominated the effects on

the sensor. Comparing with the sensor responses of sensor A at different date in Figure 28 (a), (b) and Figure 29(a), the baseline resistance increased from the first day to the 74th days, after when the sensor A was out of work. Although the adsorption of water molecule in the air is reversible, MWCNT desorption is a slow process, resulting in the increase of the baseline value. As a consequence, the water molecules accumulated on the surface of MWCNT will affect the performance of ZnO-MWCNT gas sensor.

Since the room RH was not controlled as RT, the changes of humidity may also lead the break of sensor. Sensor C was employed to be compared with sensor A in figure xx. Sensor C with less aging time (30 days) was stored in the same chamber and tested in the same experiment with sensor A. In Figure 29, the good response of sensor C confirms the accumulation of water absorption on the surface is the main element contributing to the aging of sensor A. The water molecule absorbed on the surface of MWCNT will slow down the diffusion rate of gas molecules. Moreover, the absorbed water molecule forming hydroxyl group on MOX surface affects the reaction of target gas on the surface.

In the air, the MWCNT can absorb O2 as well, which can affect the electrical characteristics of MWCNT. The Q. Huang et al. [47] did experiments for the adsorption of MWCNTs in the air, finding that the properties of CNT influenced by both water vapor and oxygen in air. Water vapor play a key role in room temperature. Therefore, the effect from O2 is not considered as important element.

6.4 Other effects for MOX-MWCNT

In this work, TiO_2 nanoparticles were employed to see the photocatalyst effect for this hetero-structure gas sensor. Figure x bellowed represents the sensitivities of TiO2-MWCNT gas sensor and ZnO- MWCNT gas sensor under three different target gases. Characteristics of sensors with different ALD temperature are compared as well. The detailed sensitivities of each kind of sensor are list in Table 4.

The TiO_2 –MWCNT (ALD 175C and 200C) show high sensitivity for methane at 10ppm, even more than 3 times than the sensitivity for benzene at 50ppm, implying a good selectivity between methane and benzene. In general, the ZnO-MWCNT gas sensor has higher sensitivity for benzene, comparing with the TiO2 –MWCNT gas sensor.

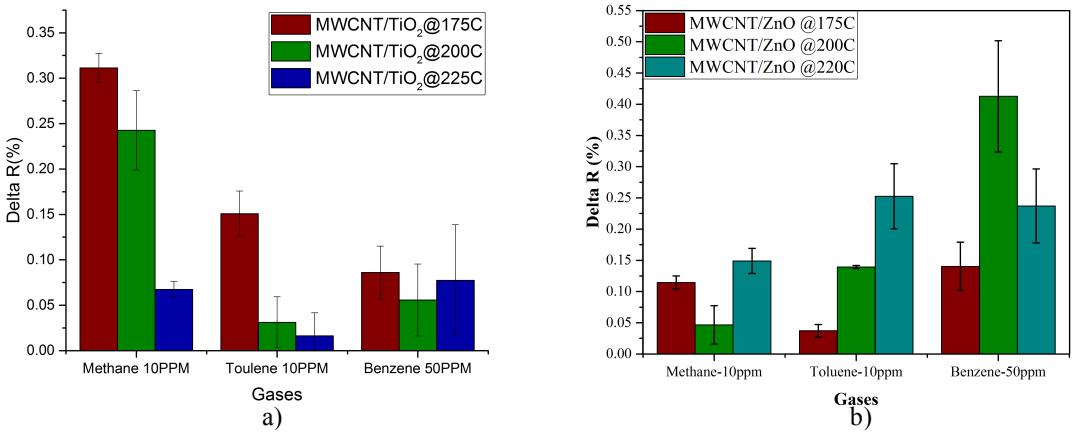

Figure 34 a) Histogram of relative resistance variation (ΔR) of TiO2-MWCNT sensor with different ALD temperatures under different target gases

b) Histogram of relative resistance variation (ΔR) of TiO2-MWCNT sensor with different ALD temperatures under different target gases

The sensitivity and selectivity under CH4, toluene and benzene are varying from different metal oxide materials and different temperature for ALD deposition. The different adhesion between MOX and MWCNTs at different deposition temperature might be the reason of this phenomenon.

Chapter 7

Conclusion

In this work, hetero-structure hydrocarbon gas sensor based on Multi-walled Carbon nanotubes functionalized with Metal Oxide nanocystals were fabricated successfully. ZnO and TiO_2 nanoparticle were deposited on the Multi-walled CNTs by ALD. The different deposition temperatures bring about the different sensitivity and selectivity for methane, toluene and benzene. Since the sensor is supposed to be applied under common conditions, the sensor ZnO-MWCNT with 175 ℃ ALD temperature were aged at RT and room RH. The accumulation of water absorption on the surface of sensor due to high adsorption and slow desorption of MWCNT is considered as the main effect of aging at common conditions. Moreover, The water in the environment increase the hydroxyl groups forming on the surface of MOX before the absorption of gas molecule affect the performance of sensor as well. The humidity is strong effect for ZnO-MWCNT (ALD 175 ℃) hydrocarbon gas sensors. In order to be operated under common conditions, a suitable method to refresh the aged senor should be explored.

Chapter 8

Future work

Since the concentration of methane used for experiments at 50% in this work was 10ppm, which was too low to see the sensor response by the interference from water molecule. The 100ppm methane can be employed in next step to get more precious data of the sensitivities at 50% RH to compare with the performance at 2% RH.

Another attractive topic is the photocatalyst selection. Characteristics and aging effects of TiO_2-MWCNT sensor can be studied and compared with ZnO-MWCNT sensor.

Bibliography

[1] J. Kesselmeier, M. Staudt, Biogenic Volatile Organic Compounds (VOC): An Overview on Emission, Physiology and Ecology, Journal of Atmospheric Chemistry [J] 1999, 5, 23-88

[2] Jin Huang, Qing Wan, Gas Sensors Based on Semiconducting Metal Oxide One-Dimensional Nanostructures, Sensors [J] 2009, 9, 9903-9924

[3] Yu-Feng Sun et, Metal Oxide Nanostructures and Their Gas Sensing Properties: A Review, Sensors [J] 2012, 12, 2610-2631

[4] Xiao Liu,1 Sitian Cheng, A Survey on Gas Sensing Technology, Sensors (Basel), 2012, 12(7): 9635–9665.

[5] Xiaoxing Zhang, Mechanism and Application of Carbon Nanotube Sensors in SF6 Decomposed Production Detection: a Review, Nanoscale Res Lett. 2017; 12: 177.

[6] M.T Humayun, R Divan, etc., Novel chemoresistive CH_4 sensor with 10ppm sensitivity based on multiwalled carbon nanotubes functionalized with SnO2 nanocrystals, Journal of Vacuum Science & Technology A 34, 2016;

[7] M. Mittal , A. Kumar . Carbon nanotube (CNT) gas sensors for emissions from fossil fuel burning, Sensors and Actuators B: Chemical [J], 2014 (11): 349-362

[8] Y.h Gui, S Li, J Xu, C Li, Study on TiO2-doped ZnO thick film gas sensors enhanced by UV light at room temperature, Microelectronics Journal [J], 2008 (9): 1120-1125

[9] Dinesh K. Aswal, Shiv K. Gupta, Science and Technology of Chemiresistor Gas Sensors.P4-P29

[10] C.x Wang, Longwei Yin, Metal Oxide Gas Sensors: Sensitivity and Influencing Factors, Sensors (Basel). 2010; 10(3): 2088–2106.

[11] Picture from http://www.edaphic.com.au/gas-detection-encyclopedia/semiconductor-sensors/

[12] K.W. Lin, C.C. Cheng, A novel Pd/oxide/GaAs metal–insulator–semiconductor field-effect transistor (MISFET) hydrogen sensor, SEMICONDUCTOR SCIENCE AND TECHNOLOG, 16 (2001) 997–1001

[13] Jack Chou, Hazardous Gas Monitors: A Practical Guide to Selection, Operation, and Applications, chapter 1: 37-45

[14] N.Barsan, D.Koziej, Metal oxide-based gas sensor research: How to?, Sensors and Actuators B: Chemical, 2007(1):18-35

[15] J Chou, Hazardous Gas Monitors: A Practical Guide to Selection, Operation, and Applications, chapter 5: 55-72

[16] J Wu, S Balasubramanian , Motion-based DNA detection using catalytic nanomotors, NATURE COMMUNICATIONS[J], 2010

[17] R W. Howarth, R Santoro, etc., Methane and the greenhouse-gas footprint of natural gas from shale formations, Climatic Change, 2011(6), 106:679

[18] Picture cited from "Monitoring of hydrocarbons and organics"

[19] Ahmod Um.ir and Yoon-Bong llahn, Metal Oxide and their Applications [B], Volume 3: 31-52

[20] Vishal Balouriaa,b, S. Samantaa, Chemiresistive gas sensing properties of nanocrystalline Co3O4 thin films, Sensors and Actuators B [J](2013) 38–45

[21] T Wang, D Huang, Z Yang, A Review on Graphene-Based Gas/Vapor Sensors with Unique Properties and Potential Applications, Nano-Micro Letters [J], 2016 (4): 95–119

[22] Han-Wen Cheng, Chemiresistive properties regulated by nanoscale curvature in molecularly-linked nanoparticle composite assembly, 2017 (11)

[23] M. Ali a, V. Cimalla, Pt/GaN Schottky diodes for hydrogen gas sensors, Sensors and Actuators B 113 (2006) 797–804

[24] C Li, Meng Lv, SnO_2 Highly Sensitive CO Gas Sensor Based on Quasi-Molecular-Imprinting Mechanism Design, Sensors 2015, 15, 3789-3800

[25] P. MITRA1* and A.K. MUKHOPADHYAY, ZnO thin film as methane sensor, BULLETIN OF THE POLISH ACADEMY OF SCIENCES ZnO thin film as methane sensor TECHNICAL SCIENCES Vol. 55, No. 3, 2007

[26] Andrea Ponzoni, Metal Oxide Gas Sensors, a Survey of Selectivity Issues Addressed at the SENSOR Lab, Brescia (Italy), Sensors (Basel). 20117(4): 714.

[27] Q. Wan, Q. H. Li, Fabrication and ethanol sensing characteristics of ZnO nanowire gas sensors, APPLIED PHYSICS LETTERS [J], 2004 (5): 18

[28] C Lin, S-J Chang, A low-temperature ZnO nanowire ethanol gas sensor prepared on plastic substrate, Materials Research Express [J], 2016 (3):9

[29] Jiwon Lee, etc., A hydrogen gas sensor employing vertically aligned TiO2 nanotube arrays prepared by template-assisted method, Sensors & Actuators: B,Chemical, 2011(1):1494-1498

[30] Liu J1, Guo Z, Meng F, Novel porous single-crystalline ZnO nanosheets fabricated by annealing ZnS(en)0.5 (en = ethylenediamine) precursor. Application in a gas sensor for indoor air contaminant detection. Nanotechnology. 2009 Mar 25;20(12):125501

[31] John H. Lehman, Mauricio Terrones, Evaluating the characteristics of multiwall carbon nanotubes, CARBON 49 (2011) 2581 – 2602

[32] Prabhakar R. Bandaru, Electrical Properties and Applications of Carbon Nanotube Structures, Journal of Nanoscience and Nanotechnology Vol.7, 1–29, 2007

[33] X Zhang, H Cui, Mechanism and Application of Carbon Nanotube Sensors in SF6Decomposed Production Detection: a Review, Nanoscale Res Lett. 2017; 12: 177

[34] M. L Terranova，S Orlanducci，M Rossi, Carbon Nanomaterials for Gas Adsorption , p 368.

[35] Y.Y.Wang, Z.Yang, Flexible gas sensors with assembled carbon nanotube thin films for DMMP vapor detection, Sensors and Actuators B: Chemical, October 2010(2): 708-714

[36] L. Valentini, Armentano, Interaction of methane with carbon nanotube thin films: role of defects and oxygen adsorption, Materials Science and Engineering C 24 (2004) 527 – 533

[37] WD Zhang and WH Zhang, Carbon Nanotubes as Active Components for Gas Sensors, ournal of Sensors, (2009), Article ID 160698, 16 page

[38] Haoshuang Gu, Hydrogen Gas Sensors Based on Semiconductor Oxide Nanostructures, Sensors (Basel). 2012; 12(5): 5517–5550.

[39] D. J. Mowbray, Computational design of chemical nanosensors: Metal doped carbon nanotubes [poster]

[40] Marcelo L. Larramendy and Sonia Soloneski, Green Nanotechnology - Overview and Further Prospects", Chapter 5:Nanostructured TiO2 Layers for Photovoltaic and Gas Sensing Applications

[41] Richard W. Johnson, A brief review of atomic layer deposition: from fundamentals to applications, Materials Today, Volume 17, Number 5 June 2014 R

[42] John J. Steel, Nanostructured Metal Oxide Thin Films for Humidity Sensors, IEEE Sensors Journal [J], 2008(8):1422-1429

[43] Litao Liu, Humidity Sensitivity of Multi-Walled Carbon Nanotube Networks Deposited by Dielectrophoresis, Sensors (Basel). 2009; 9(3): 1714–1721.

[44] Francisco solis-pomar, Growth of vertically aligned ZnO nanorods using textured ZnO films, Nanoscale Research Letters 6(1):524 2011;

[45] Chen, X. et. al, Nature Communications, 2016;

[46] Park, S. et al. ACS applied materials & interfaces, 8(4), 2805-2811.

[47] Q. Huang, etc., Effect of Oxygen adsorption on Electronic properties of Carbon nanotues, Chinese Journal of Electron Devices, vol 30, no 6, Dec 2007

[48] Picture from "AppliedSensor GmbH – Chemical gas sensors to detect contaminants"
https://www.gesundheitsindustrie-bw.de/en/article/news/appliedsensor-gmbh-chemical-gas-sensors-to-detect-contaminants/